

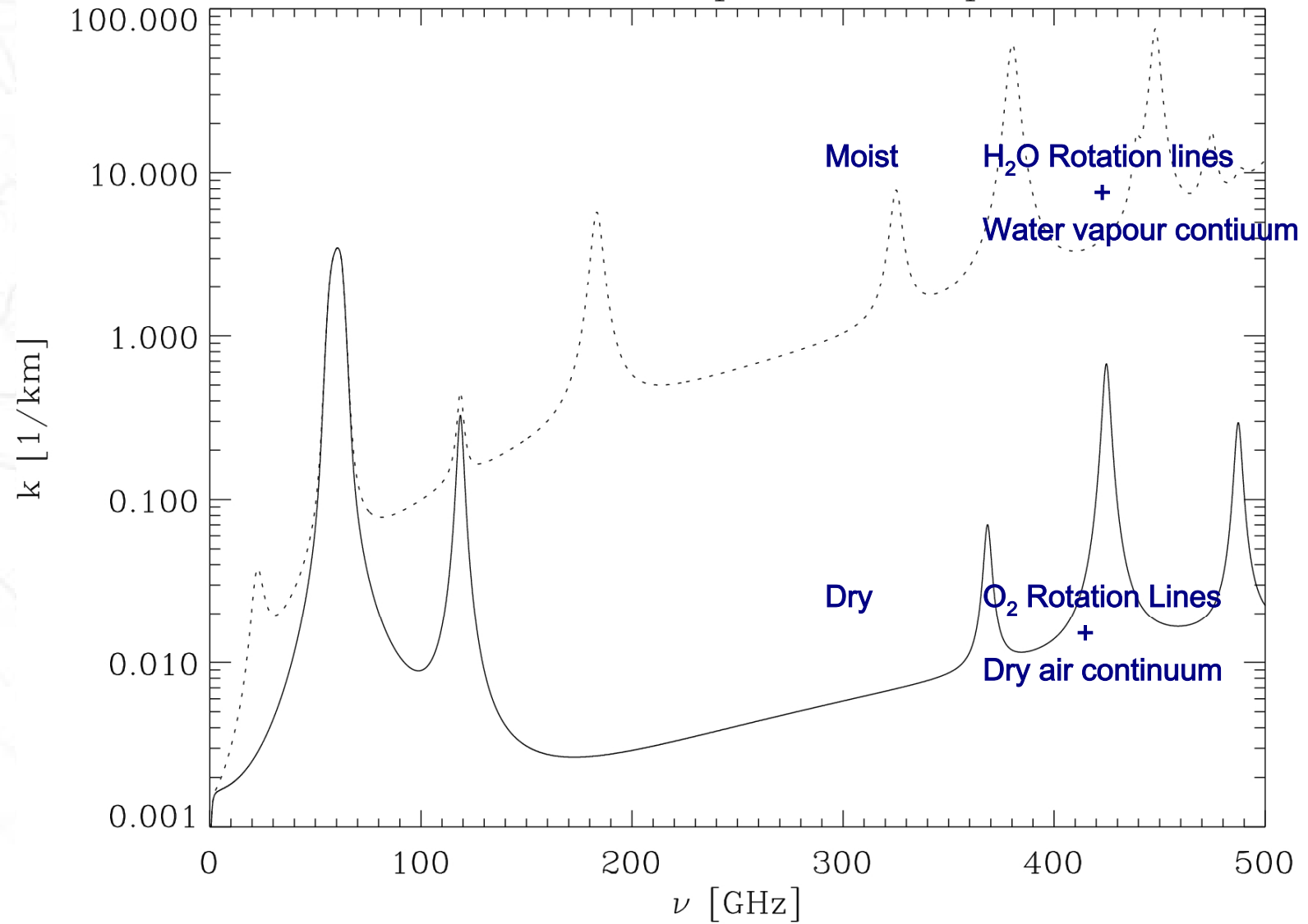
# Sources of Biases in Microwave Radiative Transfer Modelling

Peter Bauer, Sabatino Di Michele, ECMWF  
William Bell, Stephen English, The Met Office  
Christian Mätzler, University of Bern  
Ralf Bennartz, University of Wisconsin, Madison

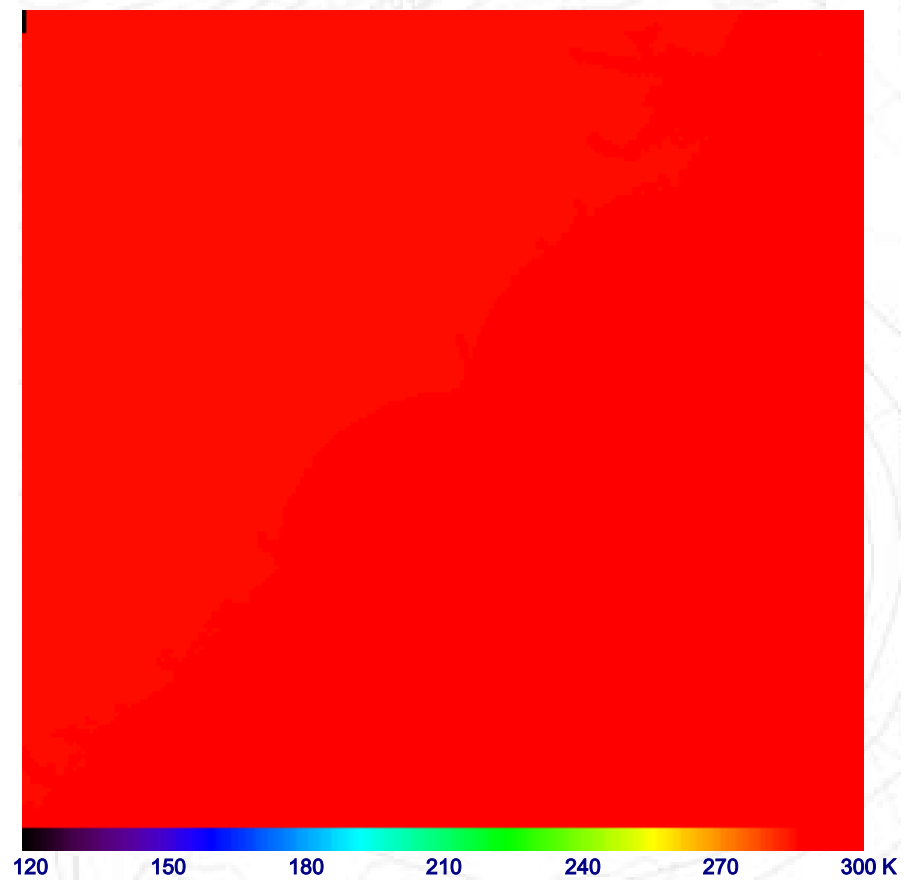
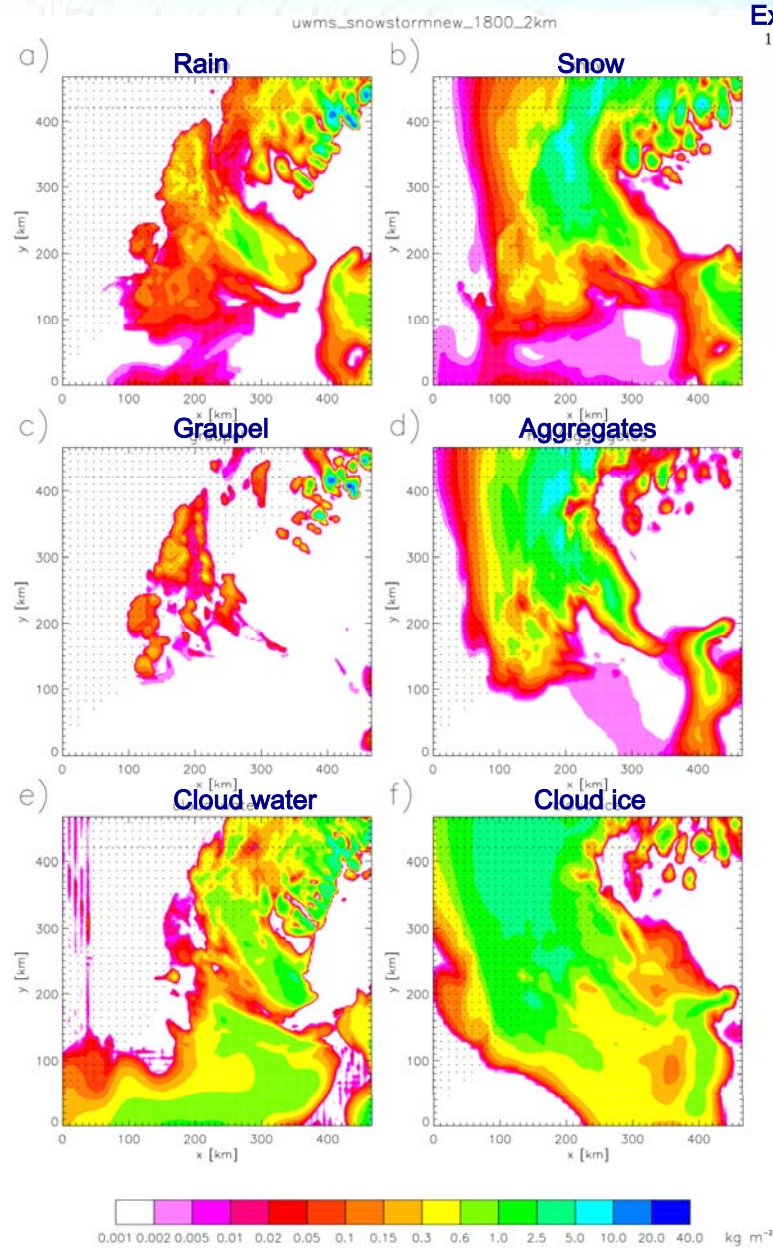
## $\mu\sim$ Spectrum

ECMWF

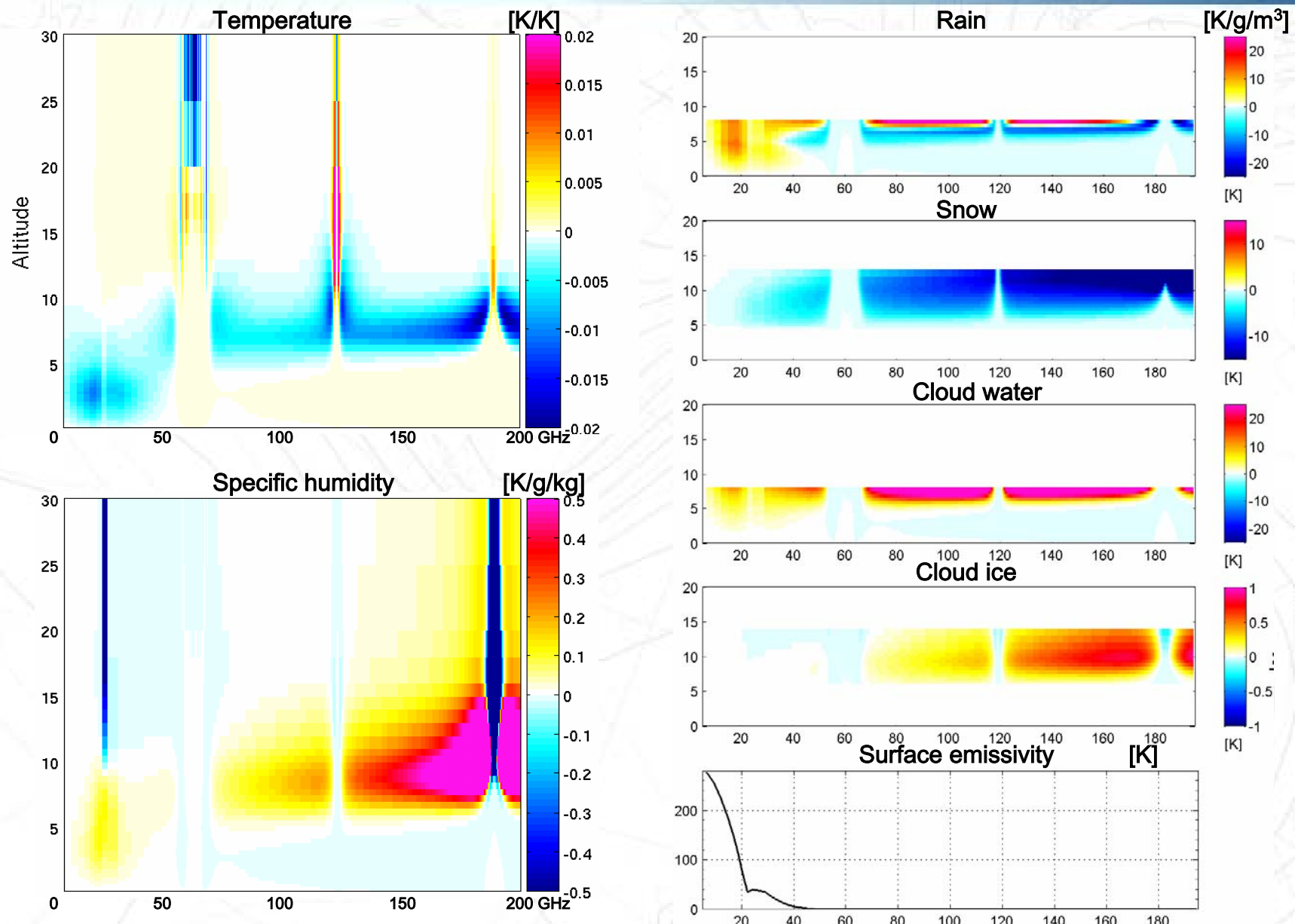
$T = 288 \text{ K}, p = 1000 \text{ hpa}$



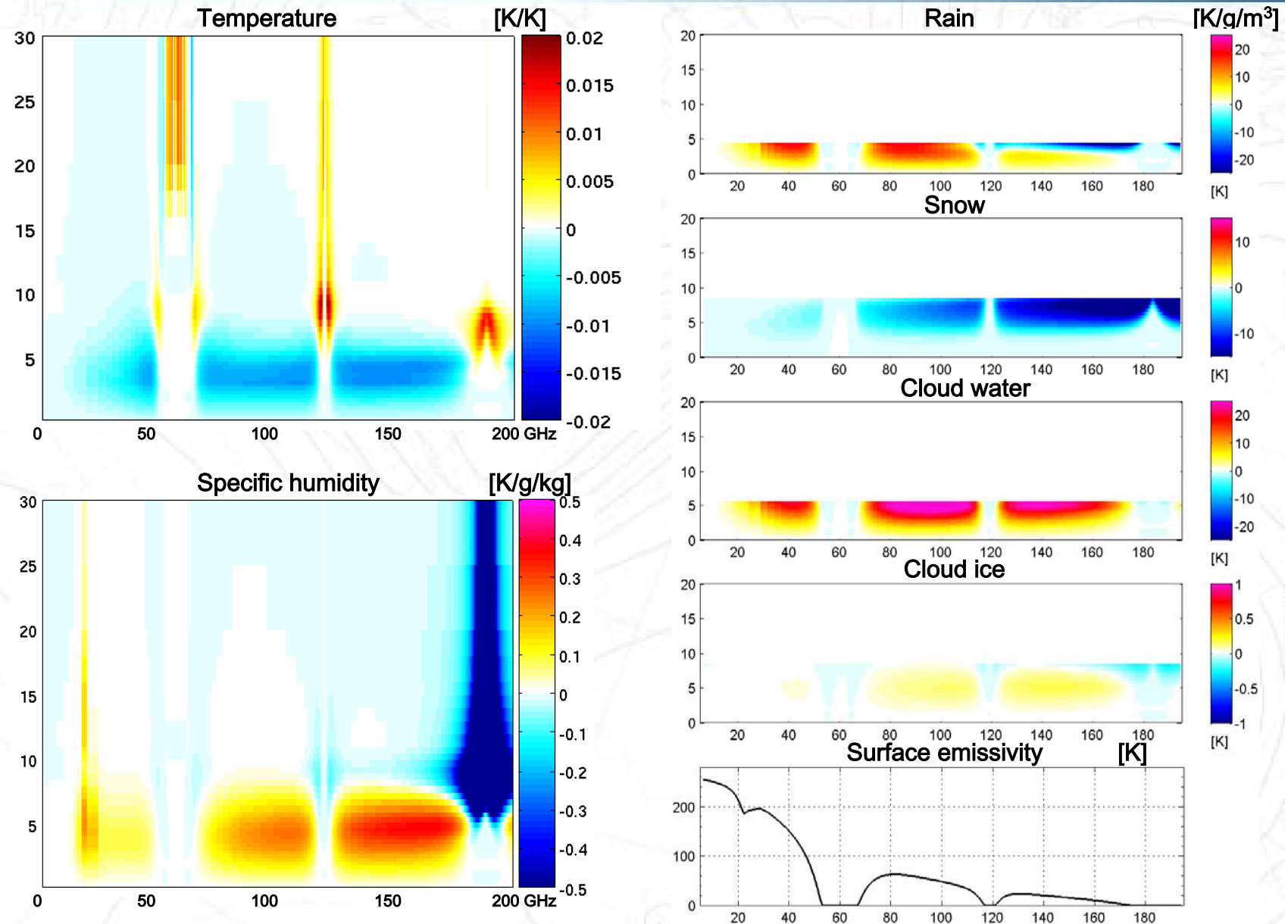
## Combined cloud-radiative transfer modelling



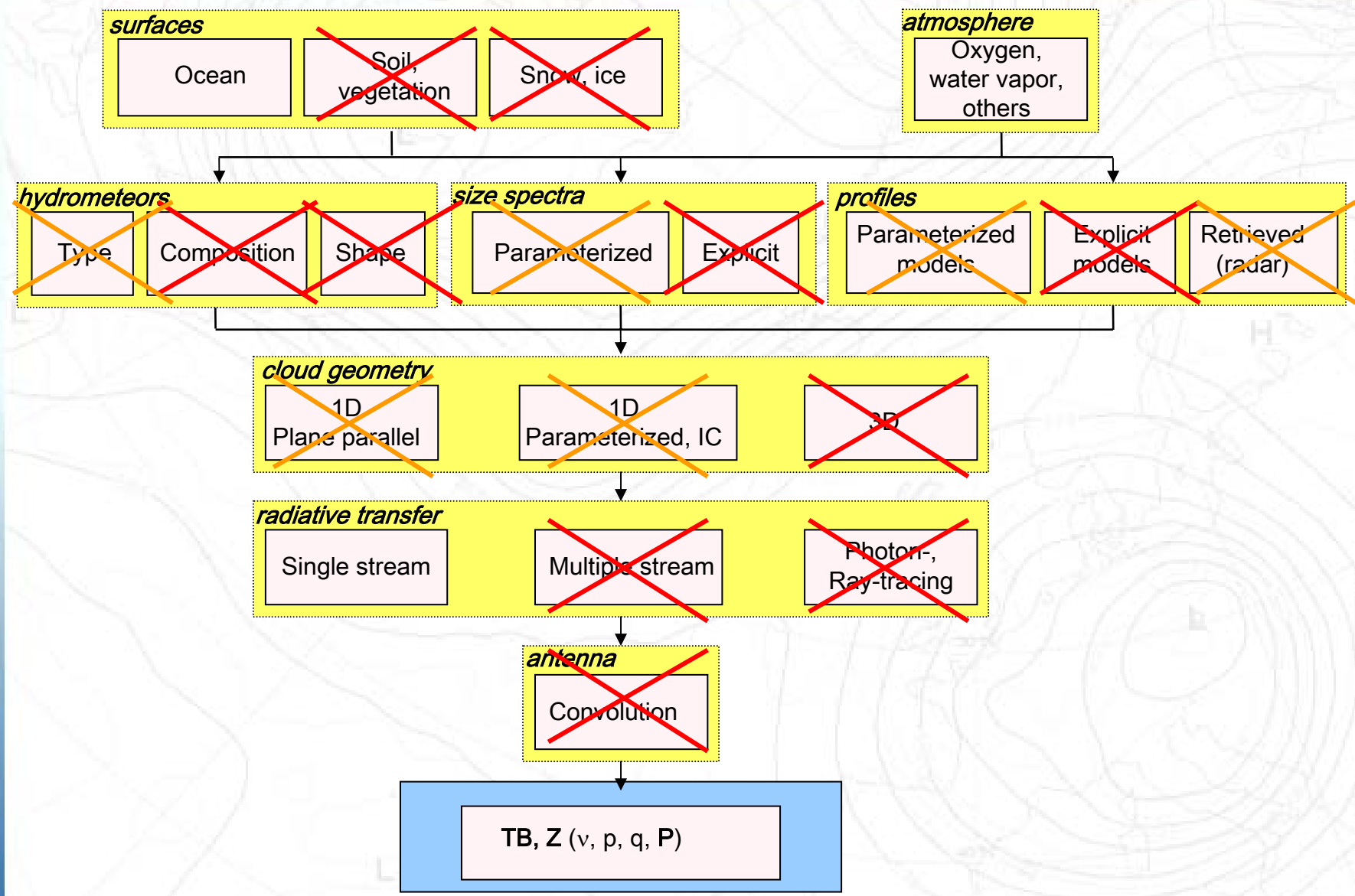
## Microwave $H_{TB}$ : Single profile over ocean



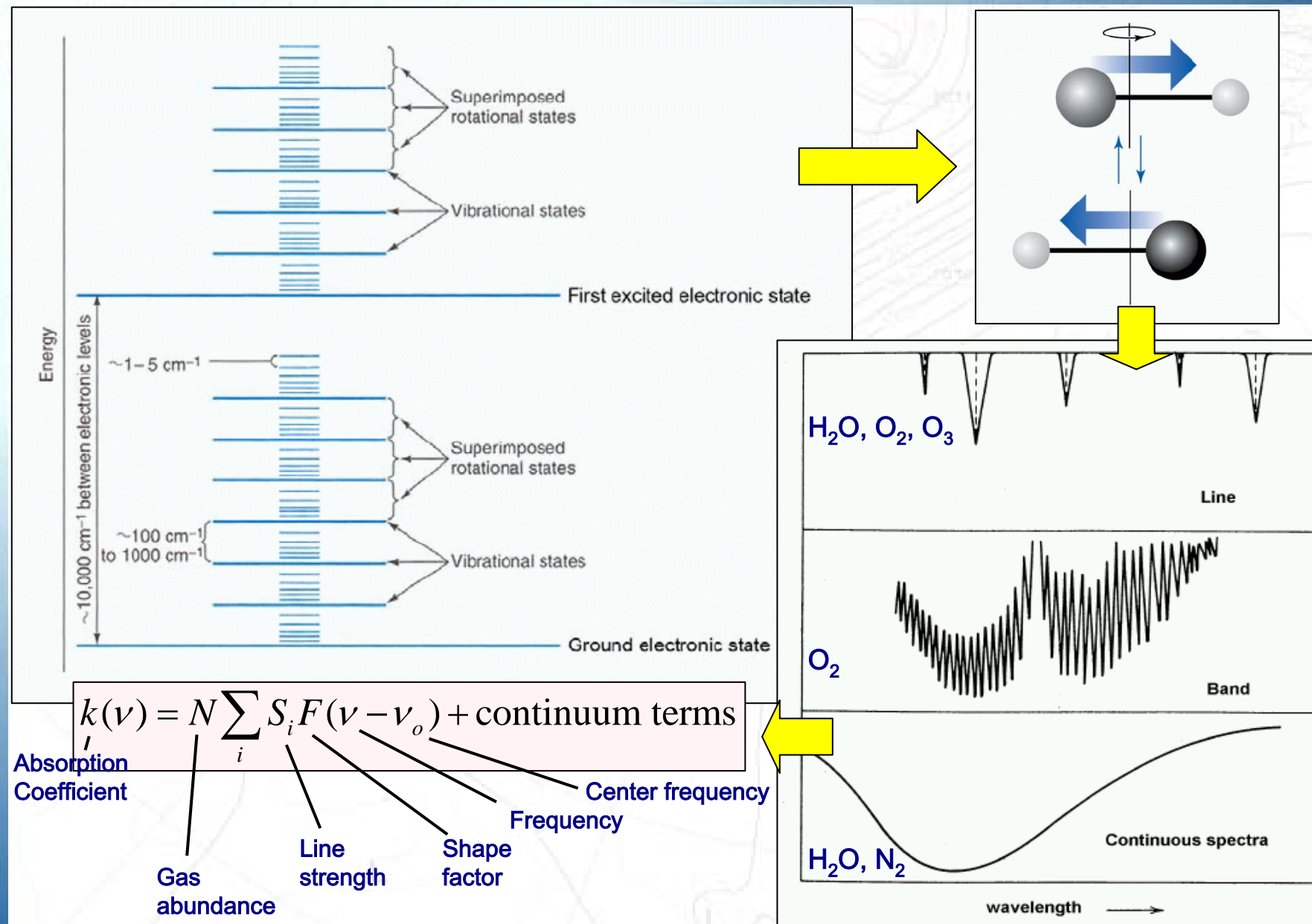
## Microwave $H_{TB}$ : Single profile over land



# Components of $\mu \sim$ RT Modelling



## Atmospheric absorption



## Inter-model evaluation



117 Profiles, RTTOV vs. LBL model

AMSU-A		RTTOV-8 117 independent set		
Channel #	NeDT degK	Mean bias degK	St. dev. degK	Max diff degK
1	0.20	0.00	0.01	0.04
2	0.24	-0.01	0.02	0.12
3	0.19	-0.02	0.03	0.18
4	0.13	0.01	0.01	0.07
5	0.13	0.02	0.01	0.08
6	0.11	0.01	0.01	0.06
7	0.12	0.00	0.01	0.03
8	0.13	0.00	0.00	0.01
9	0.15	-0.01	0.01	0.07
10	0.19	0.19	0.16	0.39
11	0.20	0.00	0.04	0.27
12	0.31	-0.02	0.07	0.44
13	0.42	-0.05	0.09	0.58
14	0.70	-0.04	0.06	0.41
15	0.10	0.07	0.10	0.34

(Saunders et al. 2005)

117 Profiles, RTTOV vs. LBL model

AMSU-B		RTTOV-8 117 independent set		
Channel #	NeDT degK	Mean bias degK	St. dev. degK	Max diff degK
1	0.32	0.07	0.10	0.33
2	0.71	-0.02	0.08	0.73
3	1.05	-0.01	0.07	0.74
4	0.69	-0.01	0.04	0.44
5	0.57	0.00	0.05	0.40

Inter-model >> LBL-parameterized  
model differences model differences

All vs.CIMSS MWLBL model

Model	AMSU-06 std bias	AMSU-10 std bias	AMSU-14 std bias	AMSU-18 std bias
RTTOV-7/8	0.04 -0.06	0.15 0.25	1.36 0.90	0.35 -0.39
OPTRAN	0.09 0.00	0.05 -0.04	0.73 -1.97	0.10 0.00
AER_OSS	0.06 0.13	0.04 0.03	0.09 0.14	0.14 -0.16
MIT	0.01 0.00	0.04 -0.04	0.08 -0.09	0.19 -0.40
RAYTHEON	<b>0.42</b> -0.57	0.17 0.24	0.20 0.60	<b>0.50</b> -0.07
AER_LBL	0.06 0.13	0.05 0.03	0.09 0.16	0.14 -0.15
MSCMWLBL	0.03 0.05	0.03 0.04	0.20 0.51	<b>0.32</b> -0.36
ATM	0.19 0.46	0.07 0.08	0.11 0.23	0.24 -0.28

## Evaluation with measurements



Table 2.8. Evolution of O<sub>2</sub> and H<sub>2</sub>O line and continuum parameters in the Millimeter-wave Propagation Model of Liebe (1977-1993). The O<sub>2</sub> parameters include line-mixing coefficients.

Year of publ.	O <sub>2</sub> parameters	H <sub>2</sub> O lines	H <sub>2</sub> O continuum
1977	M	O	O
1978	M	-	-
1981	R	O	-
1984	-	O	M
1987	-	O	M
1989	R	O	-
1992	M	-	-
1993	R	O	O

key

M: new measurements by Liebe and co-workers

R: revised analysis of earlier measurements by Liebe and co-workers

O: revision based on measurements by others

-: no change from previous version

Table 2.10. Calculated minus measured brightness-temperature differences (K) at Wallops Island, VA from England *et al.* (1993).\*

frequency, GHz	PWV	average T <sub>B</sub> , K	MPM89	W76
20.7	low	14.1	+0.38	+0.80
20.7	high	30.0	+0.15	+1.00
22.2	low	18.8	+0.56	-0.49
22.2	high	45.0	-0.76	-4.30
31.4	low	13.5	-0.33	+0.31
31.4	high	20.0	-1.10	+0.22

low PWV: <1 cm; high PWV: 2.1 cm.

Table 2.11. Calculated minus measured brightness-temperature differences (K) at Nauru Island (tropical western Pacific) from Westwater *et al.* (2003). Average PWV = 4.7 cm. The values in parentheses are 99% confidence intervals for the final digit.

frequency, GHz	average T <sub>B</sub> , K	MPM87	MPM93	R98
23.8	65	+0.80 (67)	+3.90 (70)	+0.69 (67)
31.4	32	-0.16 (32)	+3.37 (36)	+0.86 (33)

Table 2.12. Calculated minus measured 31.4-GHz brightness-temperature differences (K) at three sites, from Marchand *et al.* (2003).

location	average PWV, cm	MPM87	R98	MonoRTM
Nauru	4.0	-0.35	+0.65	-0.51
Oklahoma	1.0	-0.04	+0.42	+0.05
Alaska	0.7	-0.79	-0.34	-0.84

### Ground-based intercomparison

### Satellite data based intercomparisons

#### Meissner and Wentz (2003)

SSM/I: retrievals tuned with 19-37 GHz observations, verified against 85 GHz to within 1.2 K

#### Pumphrey and Bühler (2000)

MLS/MAS: 183 GHz line shift verified to within 0.2 MHz/torr

#### Bühler (2005)

ASUR: 626 GHz line shift verified to within 0.15 MHz/torr

#### Rosenkranz and Barnet (2005)

HSB: 0.2-0.8 K

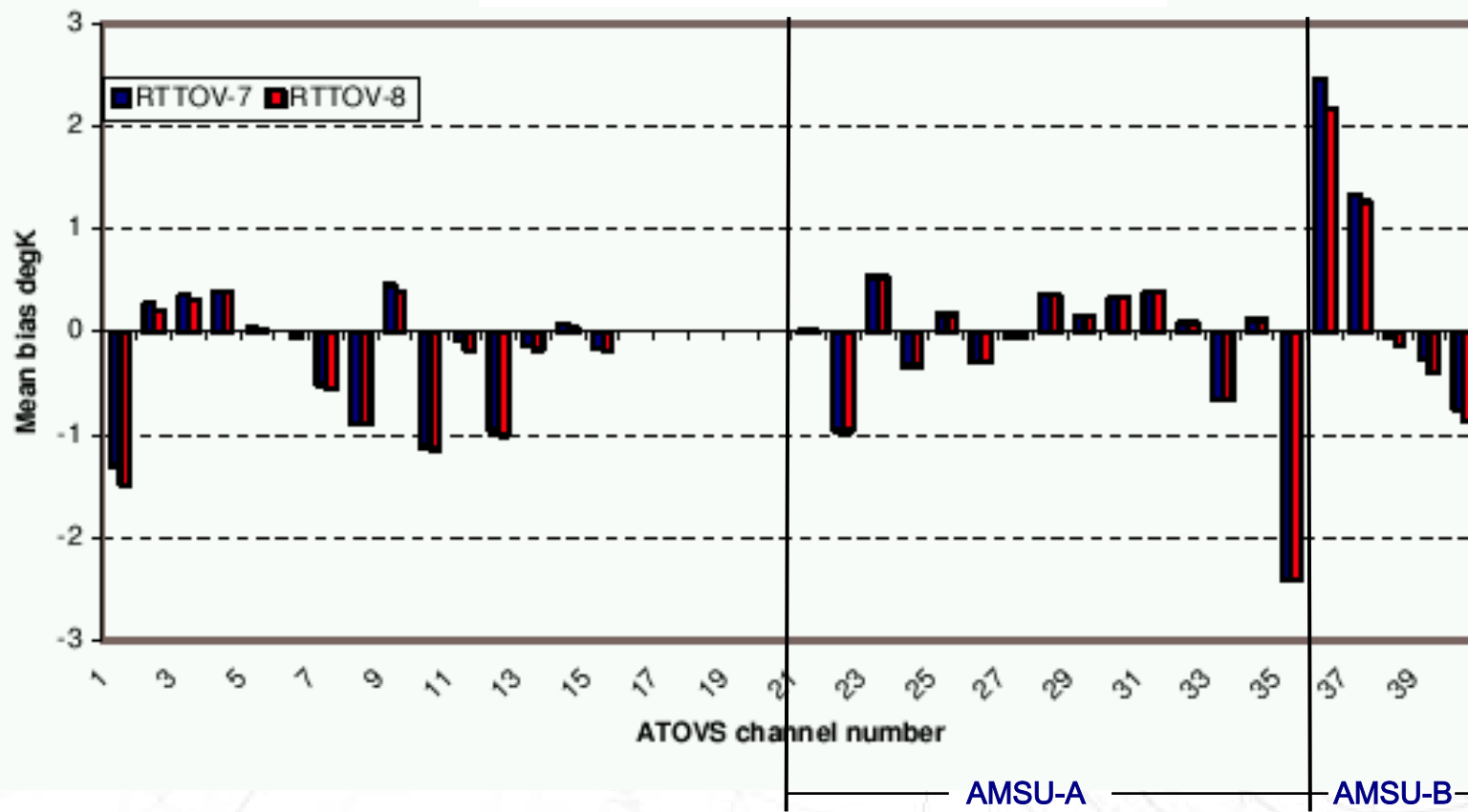
#### Rosenkranz (2003)

AMSU-A: -0.23 – 0.42 K

(Mätzler *et al.* 2005)

## Evaluation inside NWP system

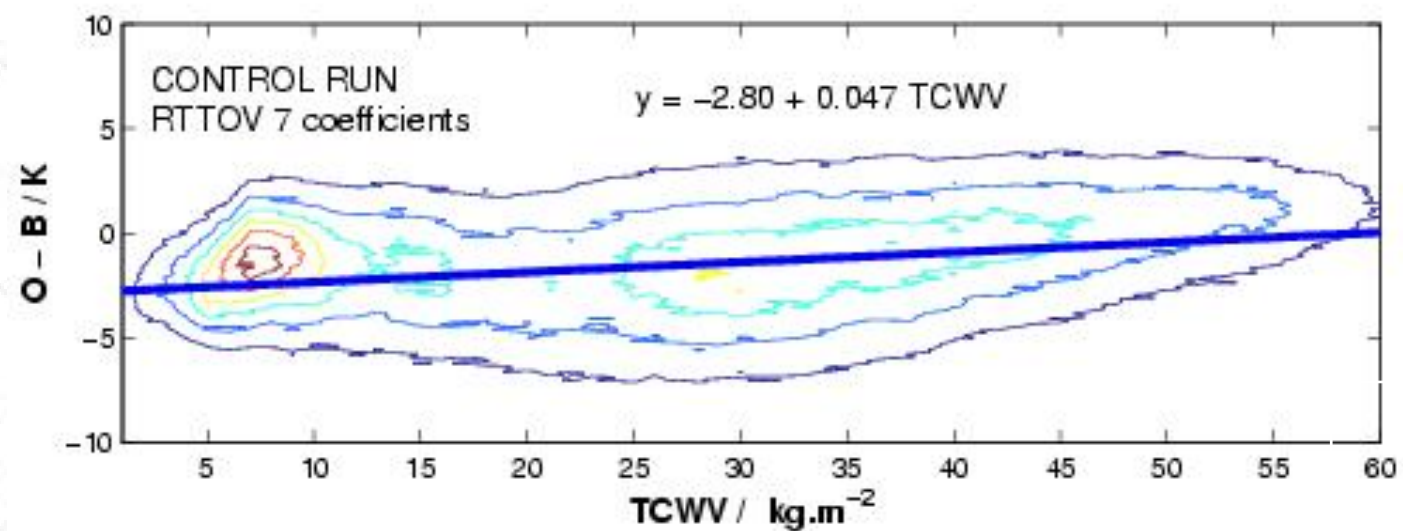
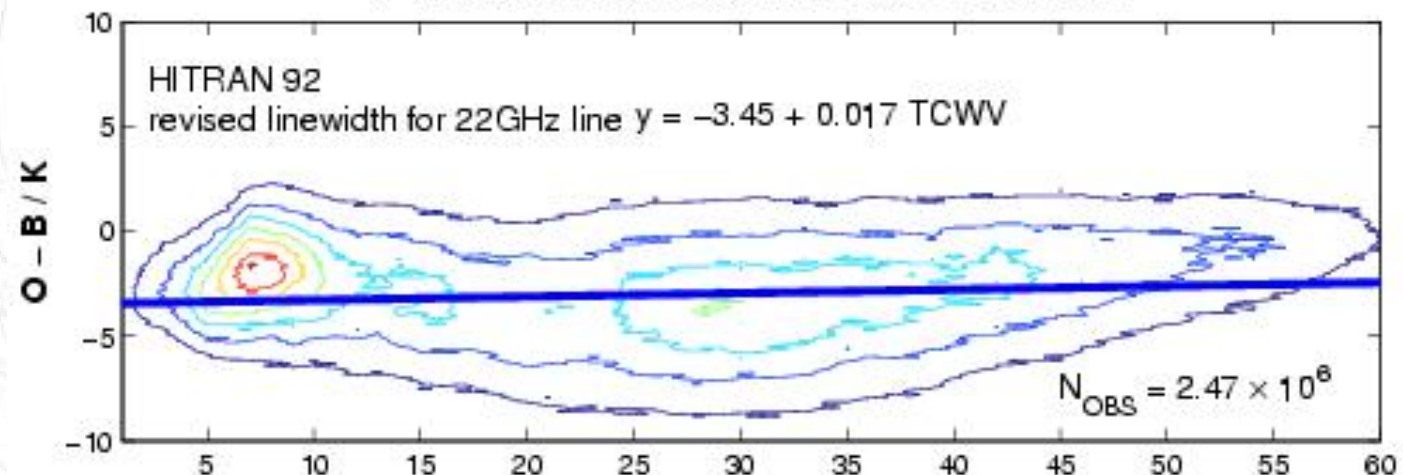
21 days O-B (ECMWF) Mean Departures



(Saunders et al. 2005)

## 22.235 GHz line-width

F13 Biases at 22GHz 18/02/05 – 08/03/05



## Issues



LBL

### Line inventory

HITRAN  
MONORTM/LBLRTM  
MPM89/92  
Rosenkranz  
ATM  
STRANSAC  
ARTS

### Pressure/temperature dependence

Natural broadening (small)  
Pressure broadening  
Doppler broadening (at low pressures)

### Continuum absorption (mainly H<sub>2</sub>O)

Photoionization (IR)  
Photodissociation (IR)  
Far wings vs. H<sub>2</sub>O clusters (MW windows)

- line intensities agree within 1%
- line frequencies accurate to within 0.1 kHz
- line widths/shifts modelling-measurements agree within a few %
- H<sub>2</sub>O continuum controversial, modelling-measurements agree within 10-20 %

All the above is function of molecule and frequency!

### Parameterizations

#### Profile datasets

Representativeness

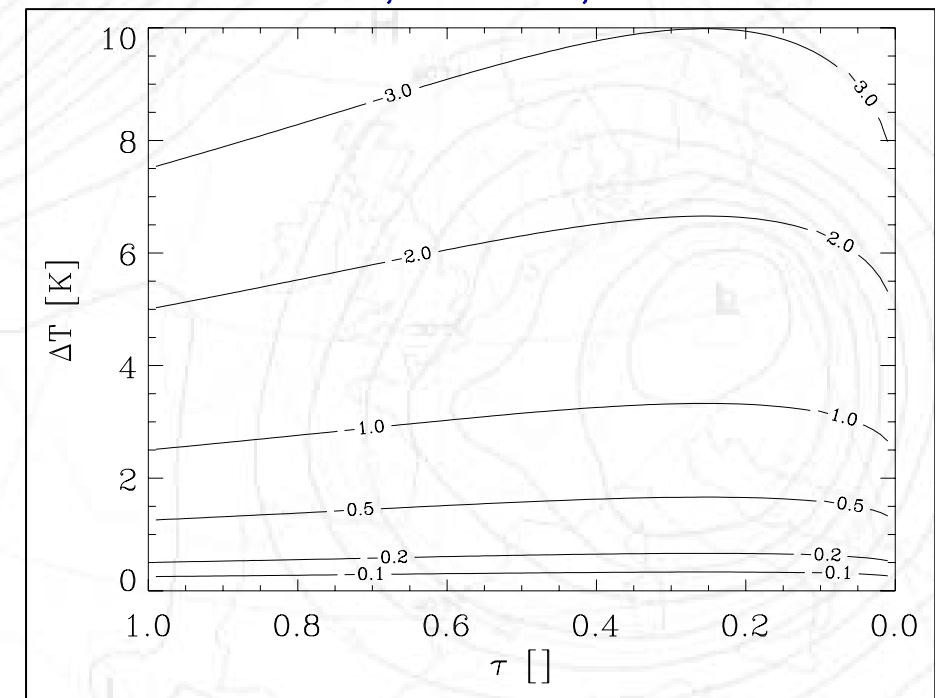
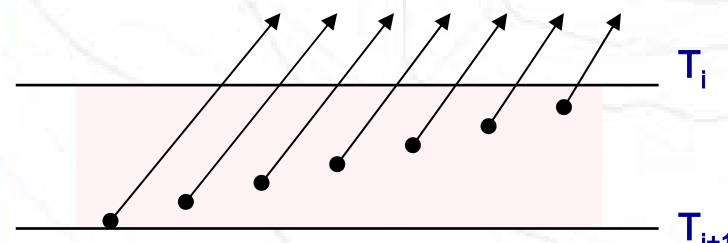
#### Predictors

Temperature, pressure, gas concentration

$$L_{\downarrow} = \int_0^{\Delta\delta} B[T(\delta)] \exp[-(\Delta\delta - \delta)/\mu] d\delta, \quad L_{\uparrow} = \int_{\Delta\delta}^0 B[T(\delta)] \exp[-\delta/\mu] d\delta$$

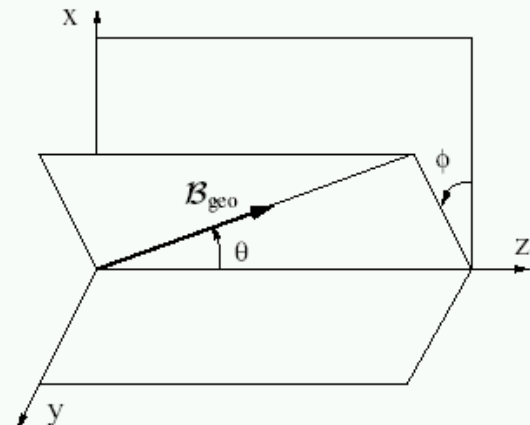
**RTTOV:**  $L_{\uparrow} = L_{\downarrow} = \frac{B(T_i) + B(T_{i+1})}{2} [1 - \tau], \quad \tau = \exp(-\Delta\delta/\mu)$

**Exact:**  $\begin{cases} L_{\uparrow} = B(T_i) - B(T_{i+1})\tau + B'[1 - \tau], & B' = \frac{B(T_{i+1}) - B(T_i)}{\Delta\delta} \\ L_{\downarrow} = B(T_{i+1}) - B(T_i)\tau - B'[1 - \tau] \end{cases}$

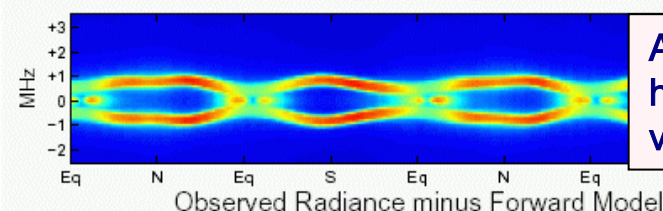
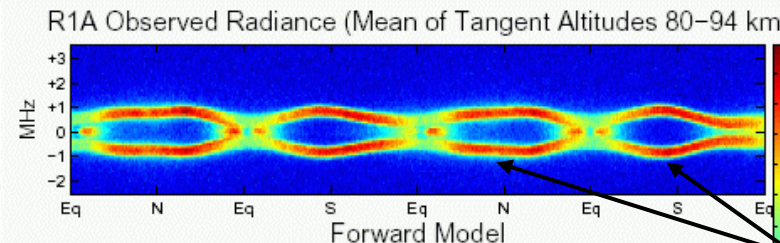


## Zeeman splitting

- Splitting of O<sub>2</sub> lines in 60 GHz band and 118.75 GHz line through interaction of O<sub>2</sub> electronic spin (with magnetic dipole moment) with Earth's magnetic field:**
- e.g. 118.75 GHz line has 3 components ( $\Delta\nu \sim 1$  MHz)
  - RT becomes polarization dependent
  - RT becomes dependent on magnetic field orientation
  - SSMIS, MLS

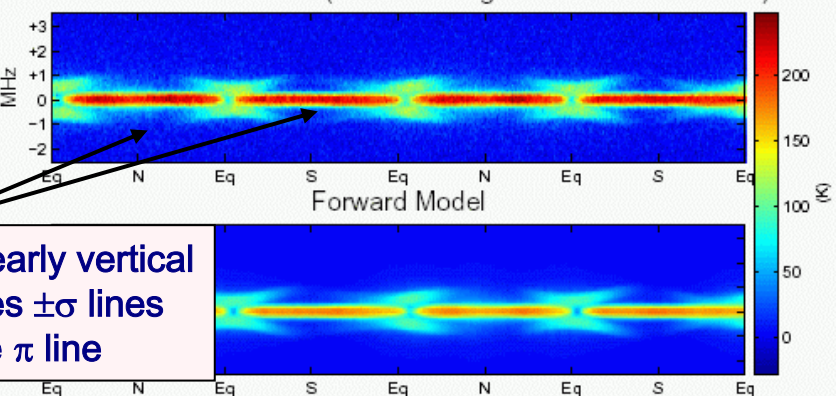


MLS Channel H<sub>h</sub> at tangent point

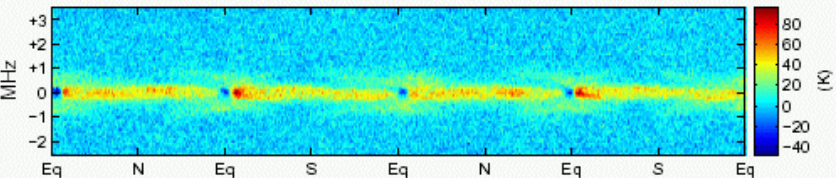
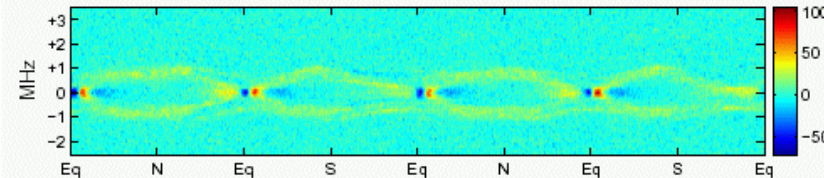


At N/S B<sub>geo</sub> nearly vertical  
h-channel sees  $\pm\sigma$  lines  
v-channel see  $\pi$  line

MLS Channel H<sub>v</sub> at tangent point



Observed Radiance minus Forward Model

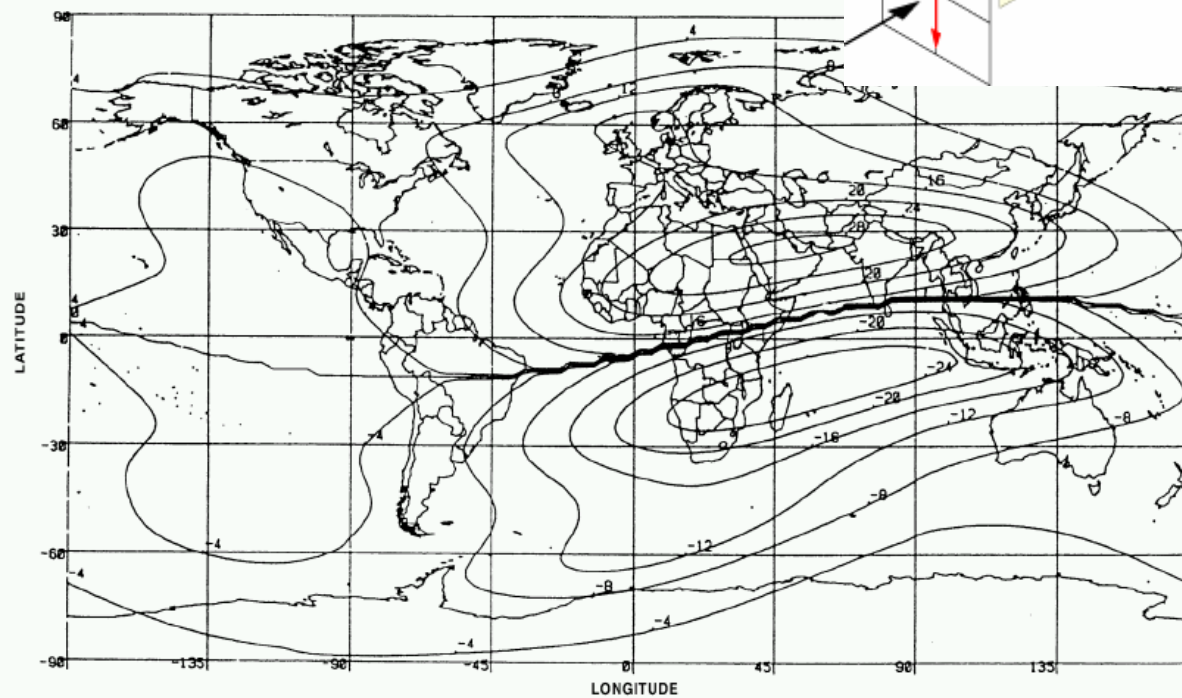
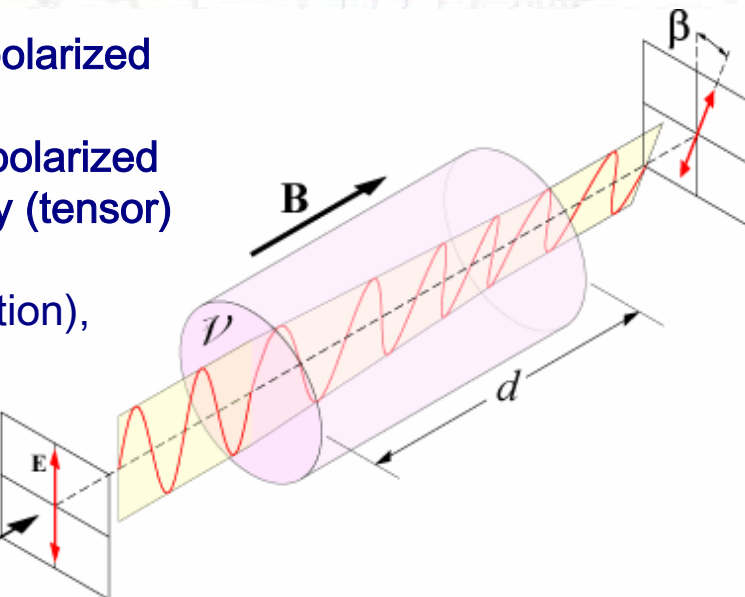


(Schwartz et al. 2005)

## Faraday Rotation

Rotation of polarization through interaction of polarized light passing through strong magnetic field (in ionosphere). Splitting of wave into 2 circularly polarized rays due to polarization dependent permeability (tensor) causing phase delay.

- affects polarized light (surface sensitive radiation), also 3<sup>rd</sup> Stokes vector
- $\beta \approx 17 / \nu^2$  ( $\beta$  in degrees,  $\nu$  in GHz)
- SMOS, AMSR, Windsat



Rotation angle simulation for 1.4 GHz  
(Svedlend 1986)

## Dielectric Properties of Natural Media



Refractive index  $n = \sqrt{\epsilon\mu} = n' + in'' = f(\text{material, frequency, temperature})$

Water permittivity models are based on Debye model + fits to observational datasets:

- 2 datasets (3-20, 30-100 GHz)
- no sea-water data above 105 GHz
- 1 dataset for 9.62 GHz for super-cooled water (-18°C)
- fits required for  $T \in [250-300 \text{ K}]$  and  $\nu \in [1, 1000 \text{ GHz}]$

Ice permittivity models are mainly based on empirical fits to observational data:

- Real part rather constant
- Imaginary part very uncertain

Snow/ice permittivity:

- From mixing formulae based on air/water/ice and inclusion shape/orientation

Vegetation permittivity:

- Mainly function of water content but complex organic structure limits applicability of conventional mixing theory
- Experimental (field) observations available but extrapolation to satellite scale and wide frequency range difficult

Soil permittivity:

- Function of frequency, temperature, and salinity, volumetric water content, volume fraction of bound and free water related to the specific soil surface area, soil bulk material, and shape of the water inclusions
- Experimental (field) observations available but extrapolation to satellite scale and wide frequency range difficult

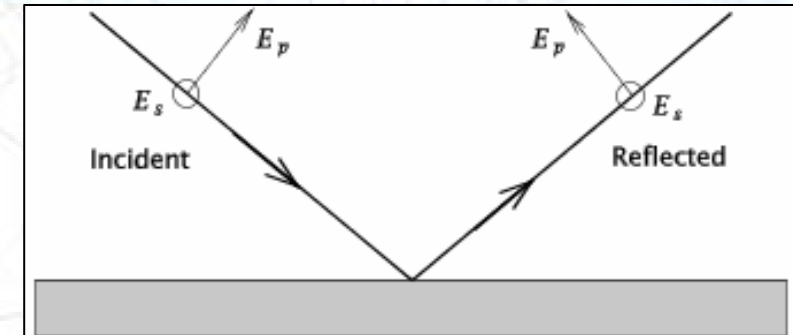
(Mätzler et al. 2005)

## Surface emissivity - Oceans



### Plane surface:

Sea-water permittivity  
Fresnel equations (I, Q)



### Wind roughened surface:

Sea-water permittivity  
Fresnel equations (I, Q)

**Large-scale waves**

Gravity-capillary, capillary waves (> 2m/s)

Whitecaps (> 7 m/s)

Foam (> 10-12 m/s)

RTTOV FASTEM-2

### Directional wind roughened surface:

Sea-water permittivity  
Fresnel equations (I, Q, U, V)

**Large-scale waves**

Gravity-capillary, capillary waves (> 2m/s)

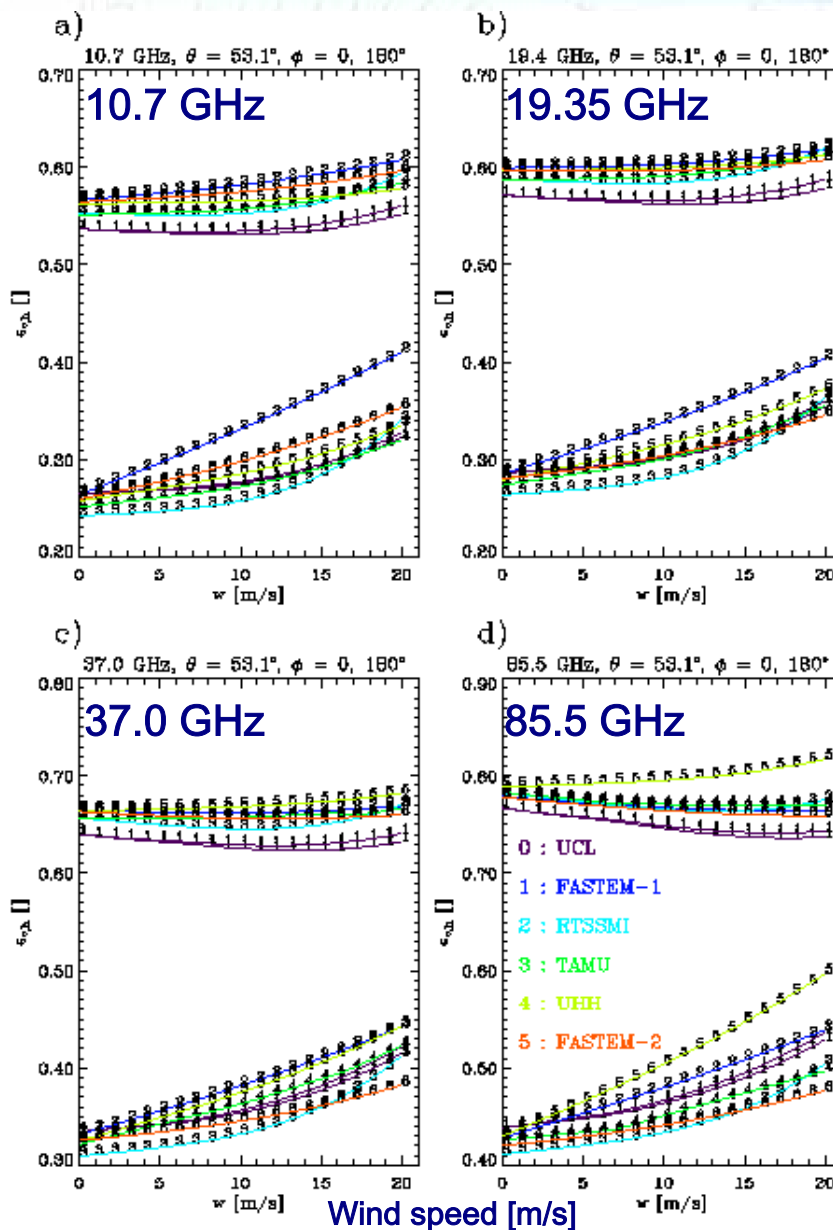
Whitecaps (> 7 m/s)

Foam (> 10-12 m/s)

RTTOV FASTEM-3

$$\mathbf{L} = \begin{pmatrix} I \\ Q \\ U \\ V \end{pmatrix} = \frac{1}{2\sqrt{\mu/\epsilon}} \begin{pmatrix} \langle E_v E_v^* \rangle + \langle E_h E_h^* \rangle \\ \langle E_v E_v^* \rangle - \langle E_h E_h^* \rangle \\ 2 \operatorname{Re} \langle E_v E_h^* \rangle \\ 2 \operatorname{Im} \langle E_v E_h^* \rangle \end{pmatrix} \approx \begin{pmatrix} I_o + I_1 \cos \varphi + I_2 \cos 2\varphi + \dots \\ Q_o + Q_1 \cos \varphi + Q_2 \cos 2\varphi + \dots \\ U_1 \sin \varphi + U_2 \sin 2\varphi + \dots \\ V_1 \sin \varphi + V_2 \sin 2\varphi + \dots \end{pmatrix}$$

## Modelled emissivity - Oceans



$\theta = 53.1^\circ$   
 $\phi = 0, 180^\circ$   
v-pol.

h-pol.

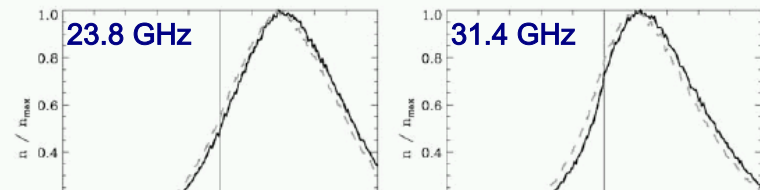
Sensitivity of surface emission ( $E_0 T_s$ ) to real and imaginary part of dielectric constant  
(Meissner and Wentz 2004)

$v$ [GHz]	$\frac{\Delta(E_0 T_s)}{\Delta \text{Re}(\epsilon)}$ $ _{T_s=273.15K}$ [K]	$\frac{\Delta(E_0 T_s)}{\Delta \text{Im}(\epsilon)}$ $ _{T_s=273.15K}$ [K]
19.35	-0.056	+1.571
37.0	+0.300	-2.705
85.5	+0.082	+4.470

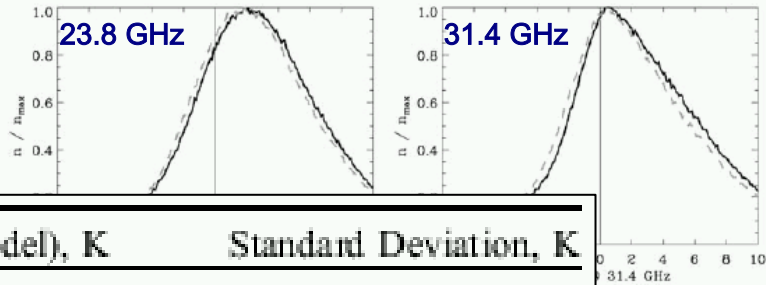
## AMSU-A FG Departures - Oceans

**ECMWF**

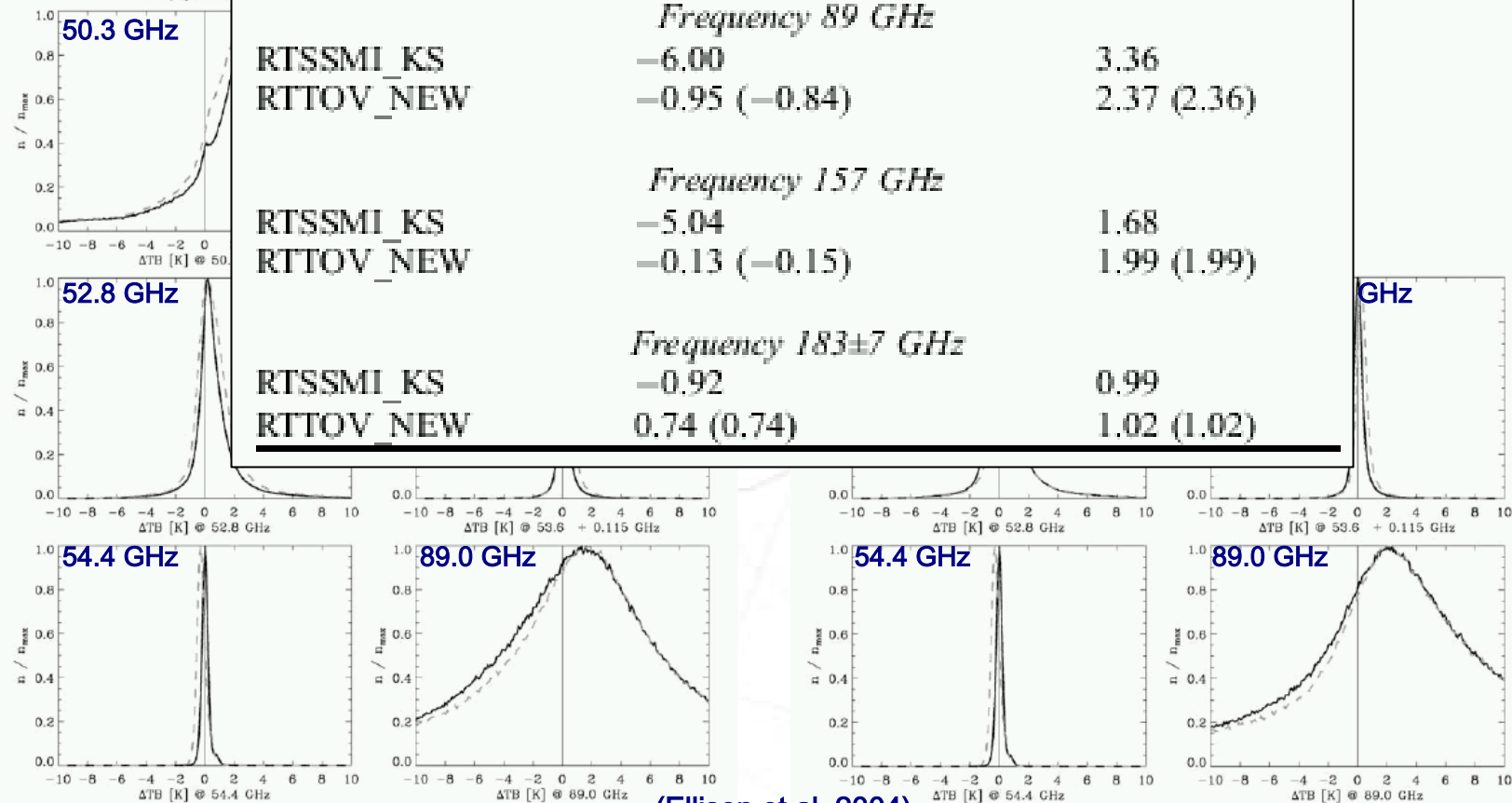
NOAA-16 AMSU-A before FASTEM-2



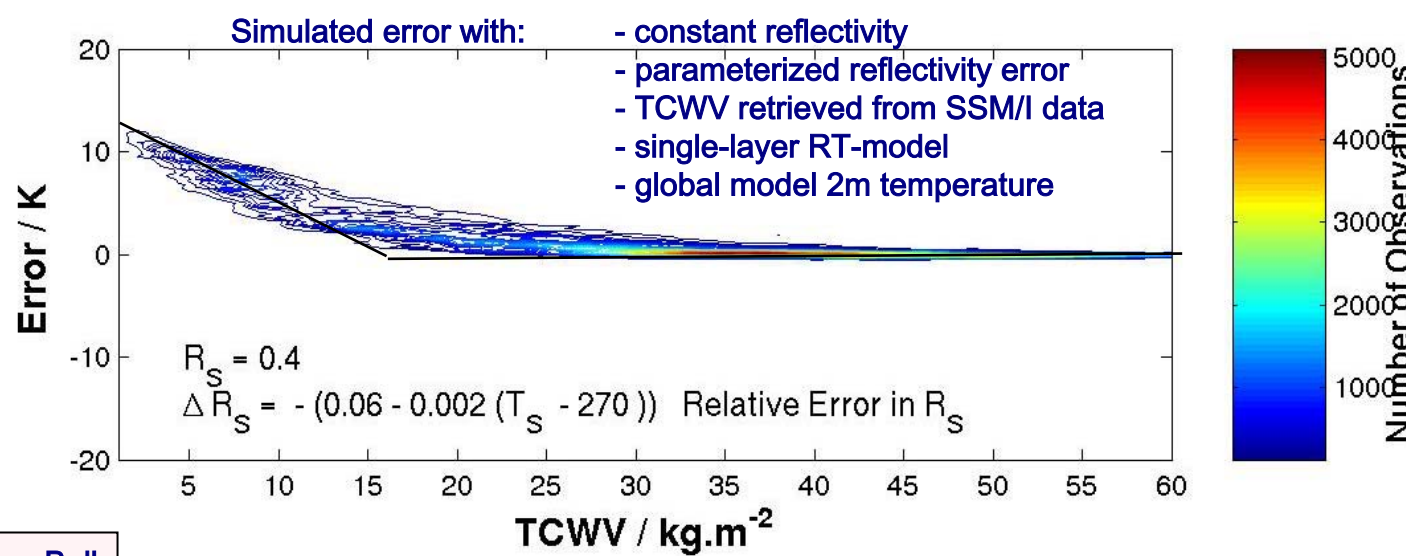
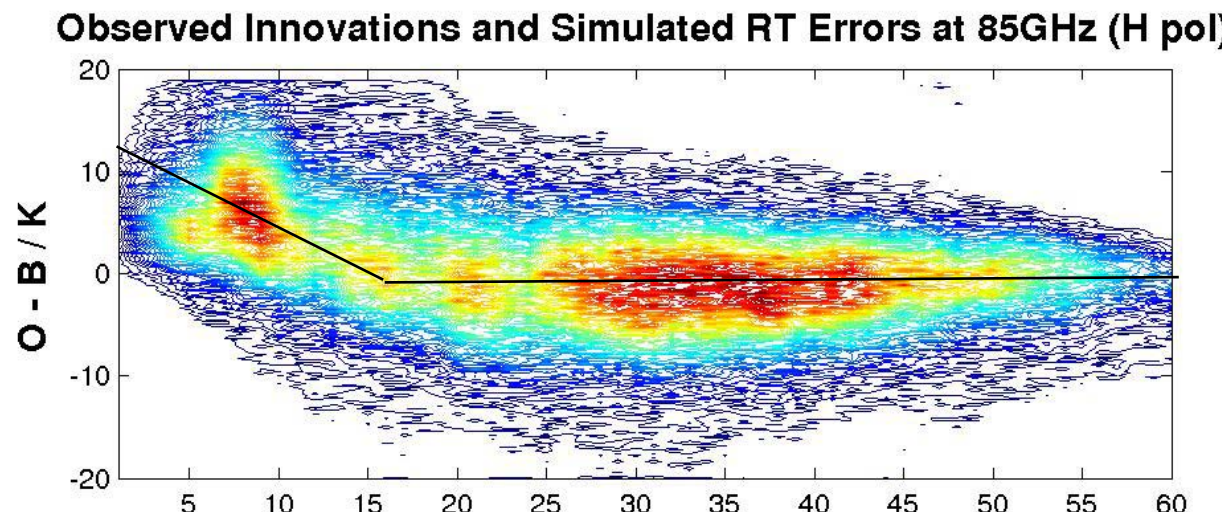
NOAA-16 AMSU-A after FASTEM-2



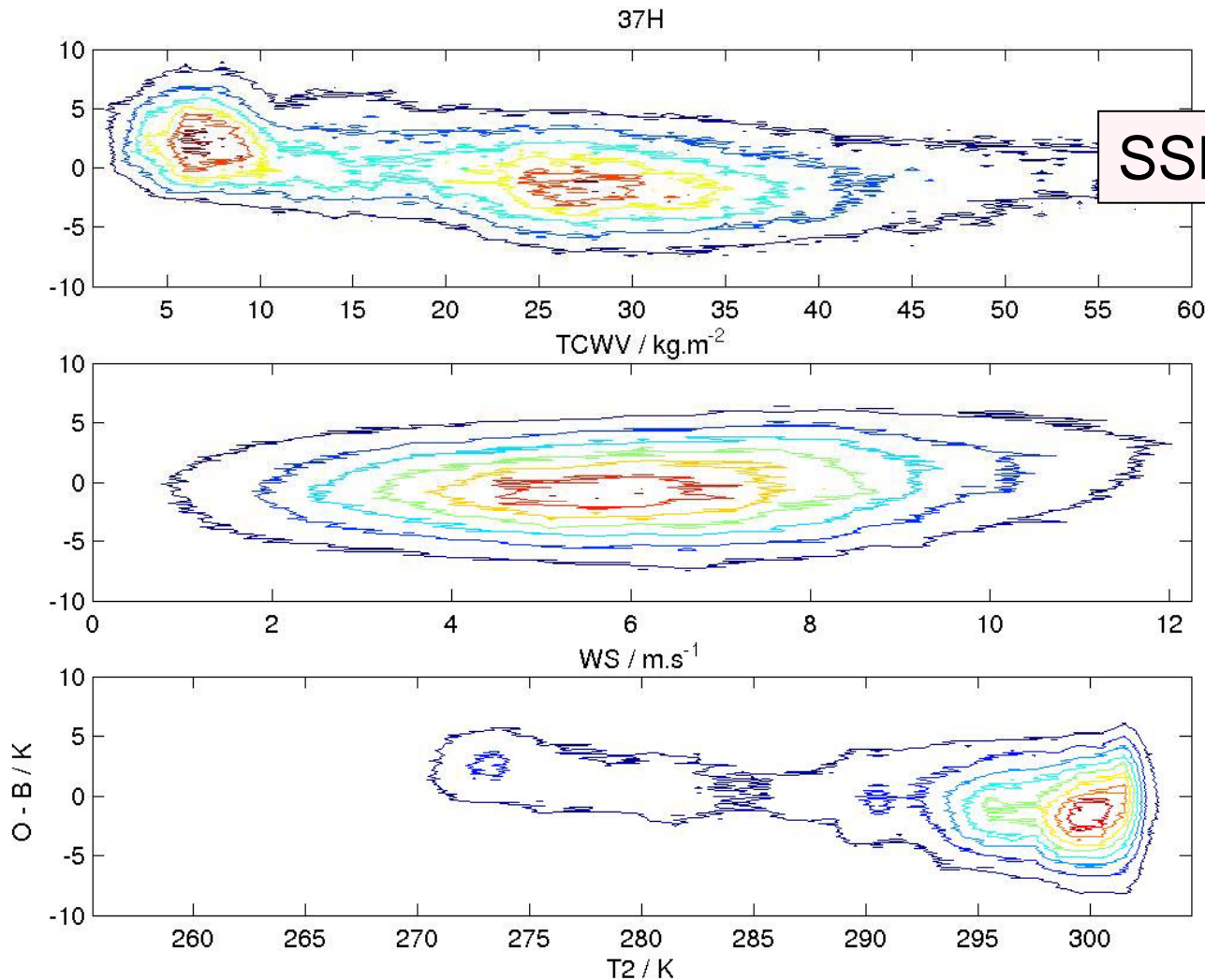
Model	Bias (Obs.-Model), K	Standard Deviation, K
<i>Frequency 89 GHz</i>		
RTSSMI_KS	-6.00	3.36
RTTOV_NEW	-0.95 (-0.84)	2.37 (2.36)
<i>Frequency 157 GHz</i>		
RTSSMI_KS	-5.04	1.68
RTTOV_NEW	-0.13 (-0.15)	1.99 (1.99)
<i>Frequency 183±7 GHz</i>		
RTSSMI_KS	-0.92	0.99
RTTOV_NEW	0.74 (0.74)	1.02 (1.02)



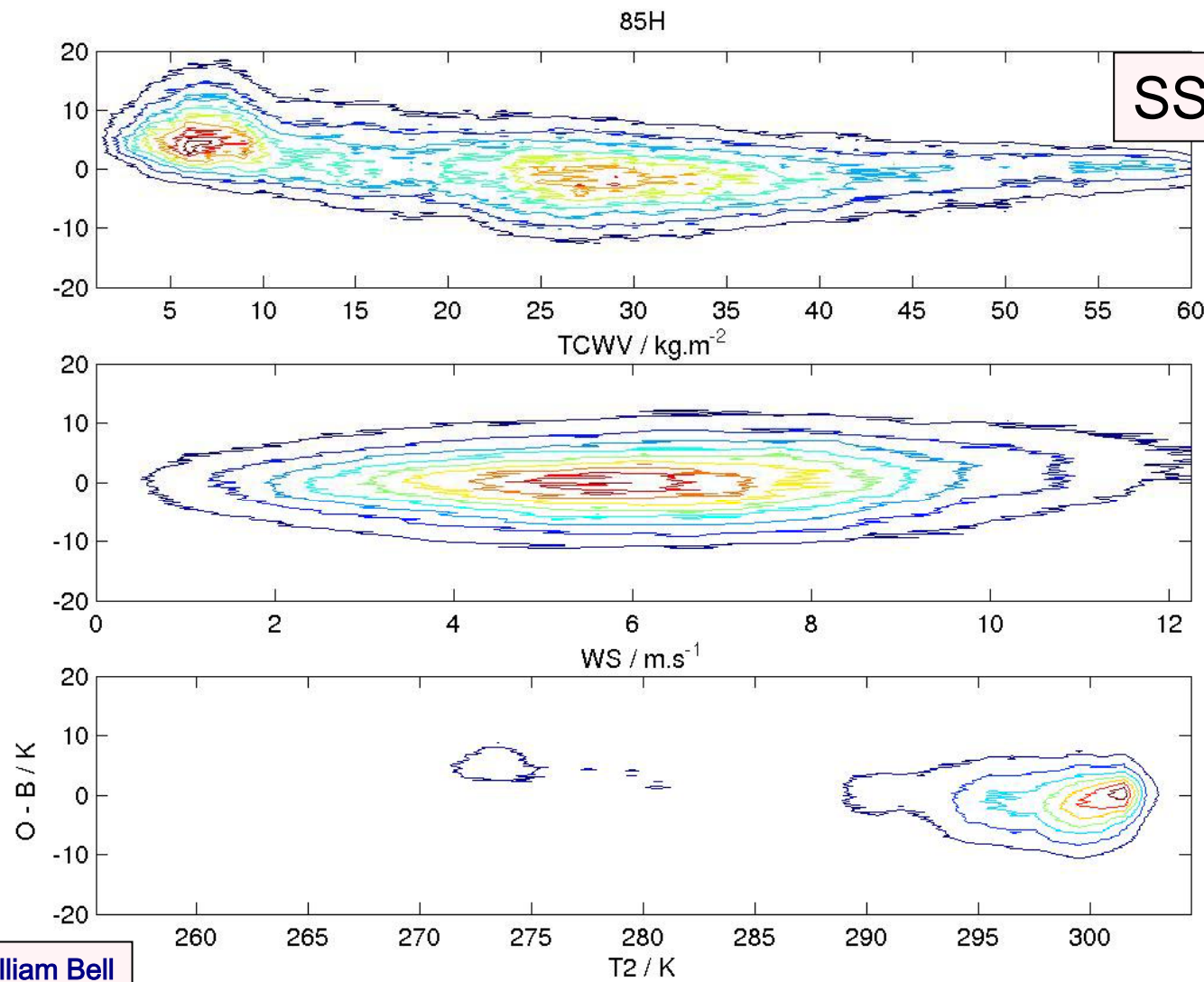
## SSM/I FG-Departure bias in dry/cold environments



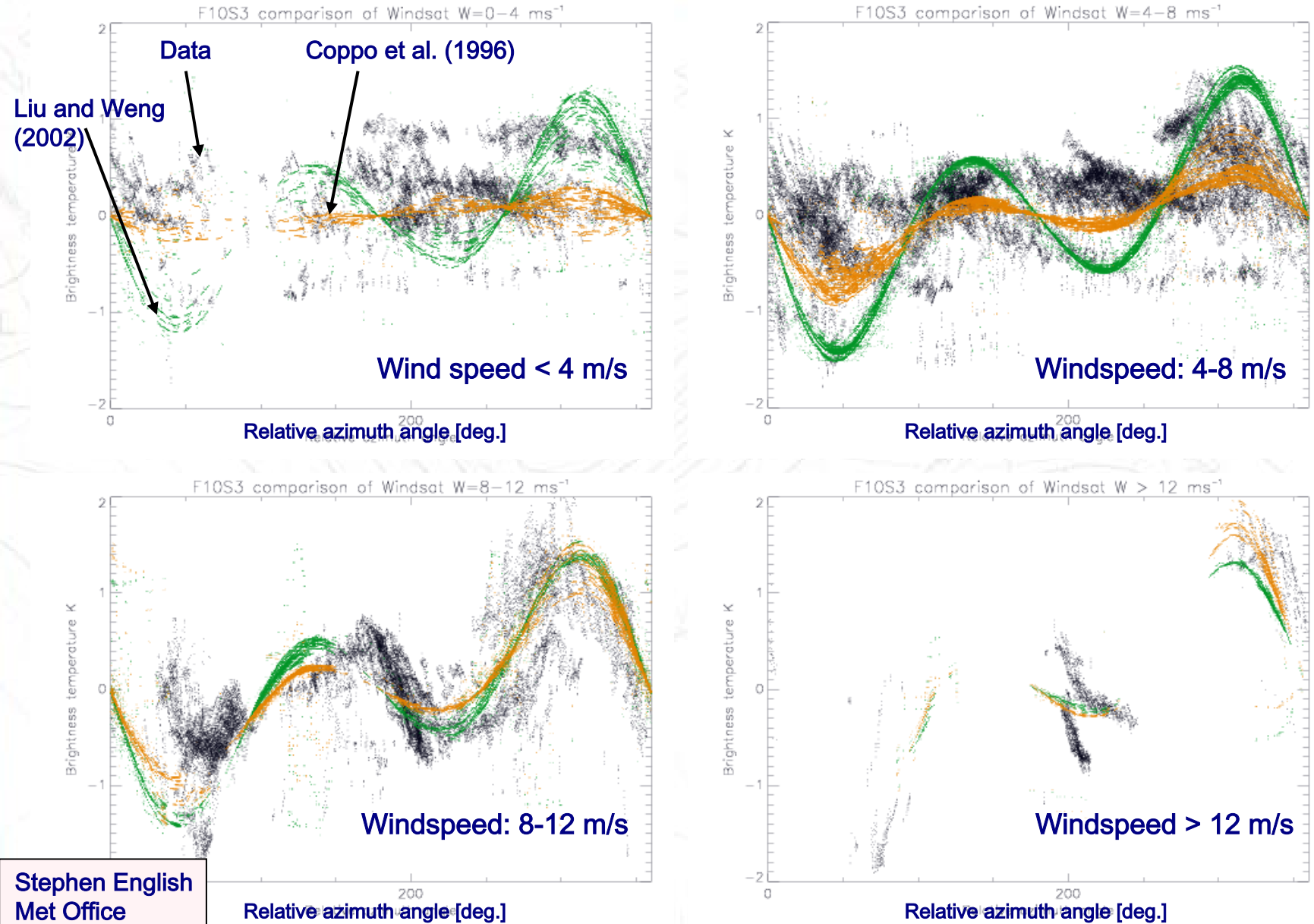
## Bias at low T: 37 GHz H pol



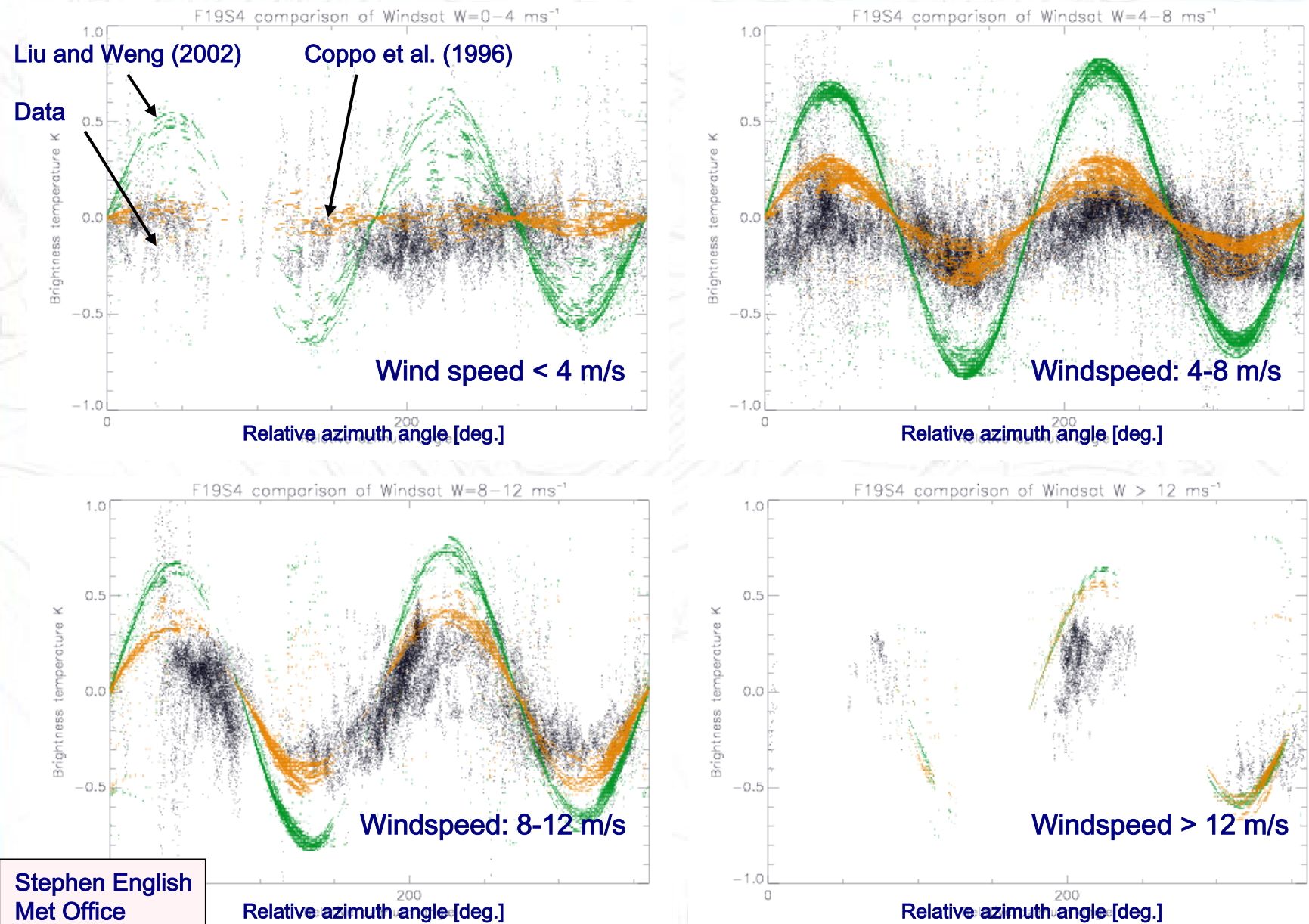
## Bias at low T: 85 GHz H pol



## 3<sup>rd</sup> Stokes Vector at 10.7 GHz: Models vs. Windsat Data

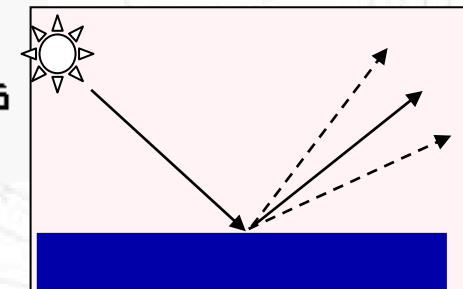
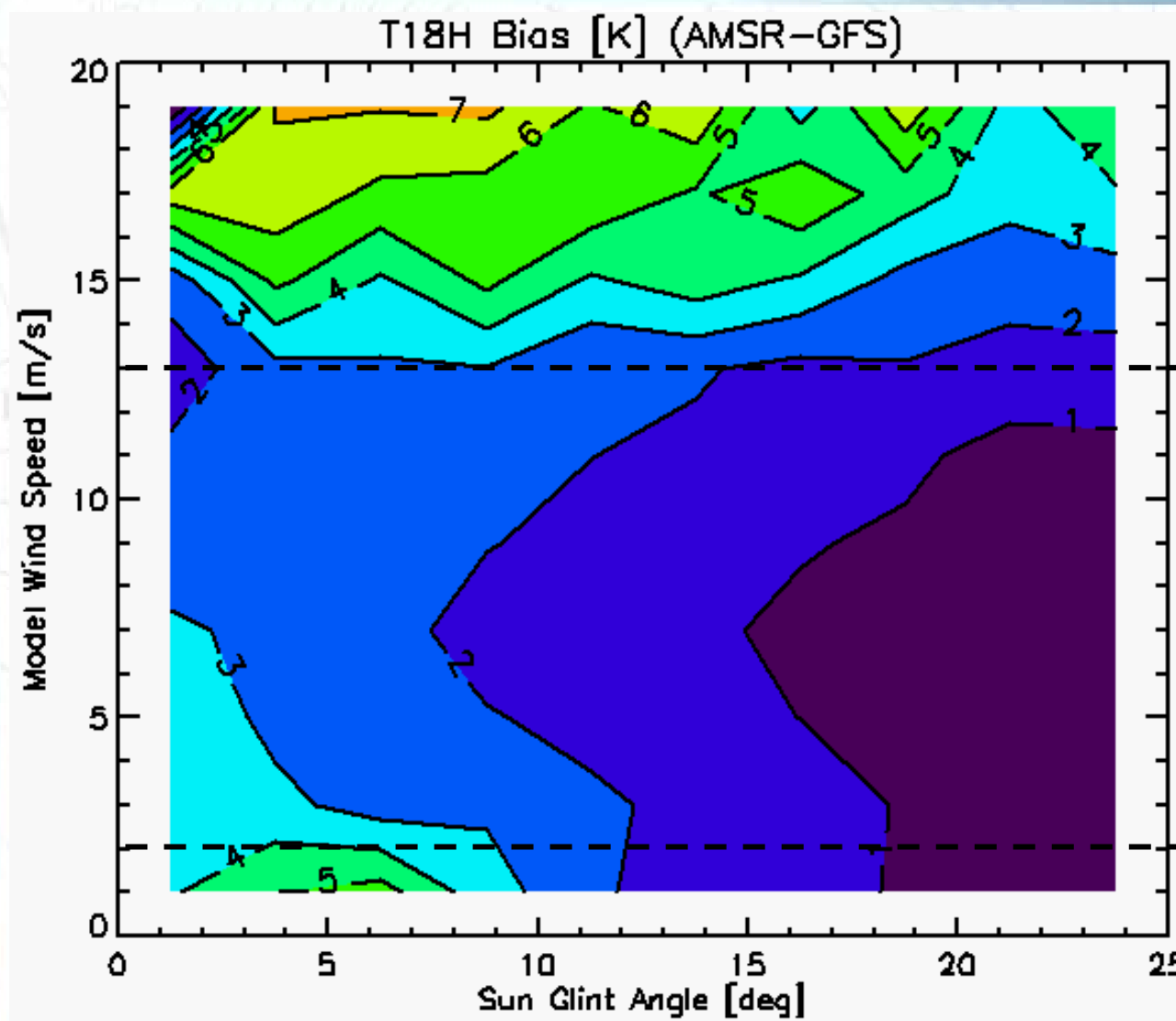


## 4<sup>th</sup> Stokes Vector at 19.35 GHz: Models vs. Windsat Data



## Sun-glint

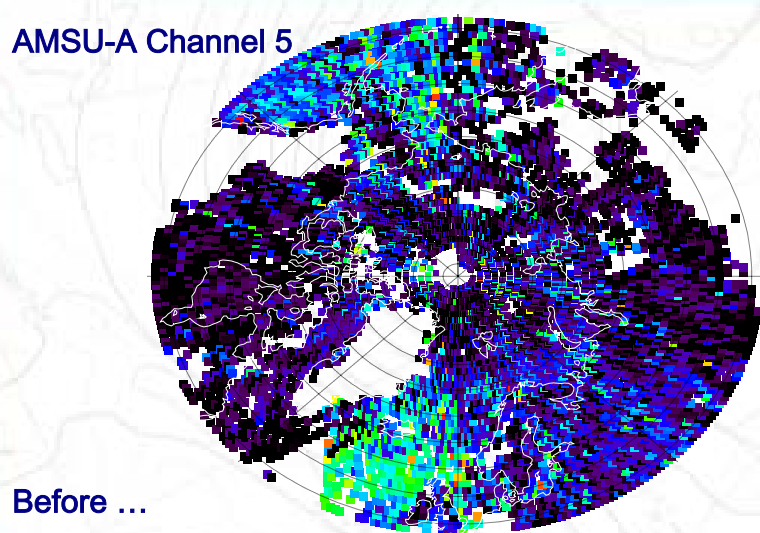
ECMWF



## Surface emission - Land

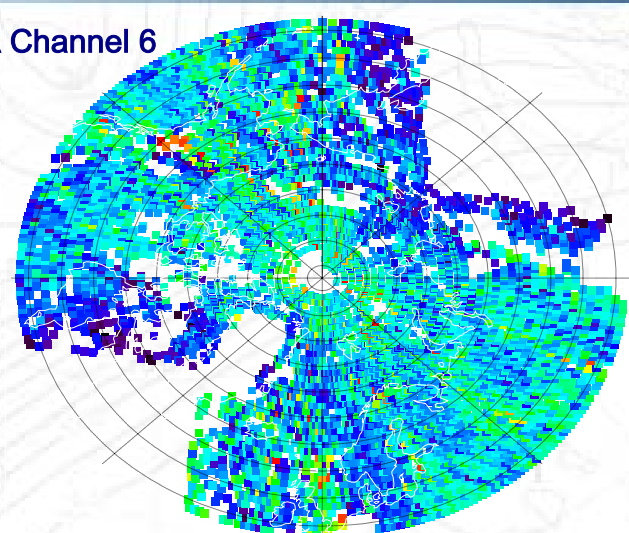
ECMWF

AMSU-A Channel 5

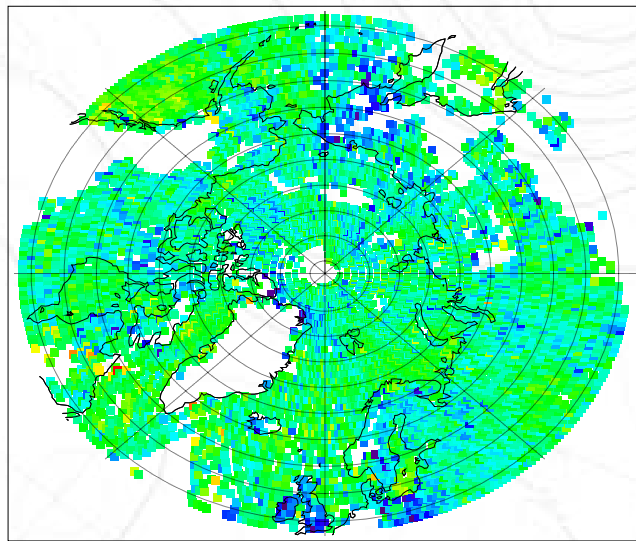


Before ...

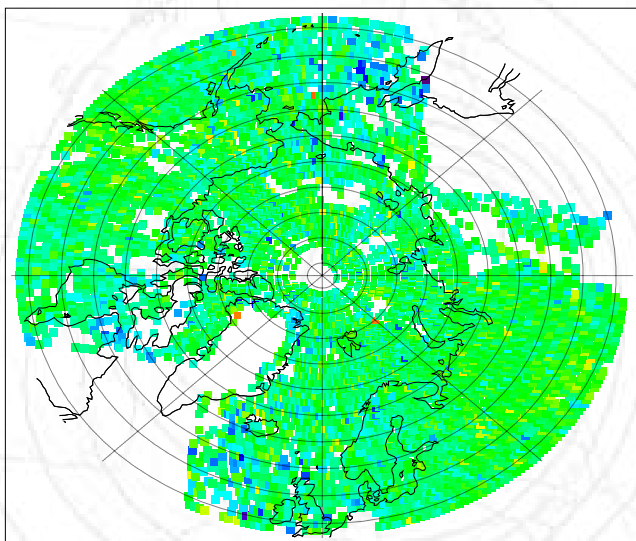
AMSU-A Channel 6



... after bias correction



Used data 20050801-03

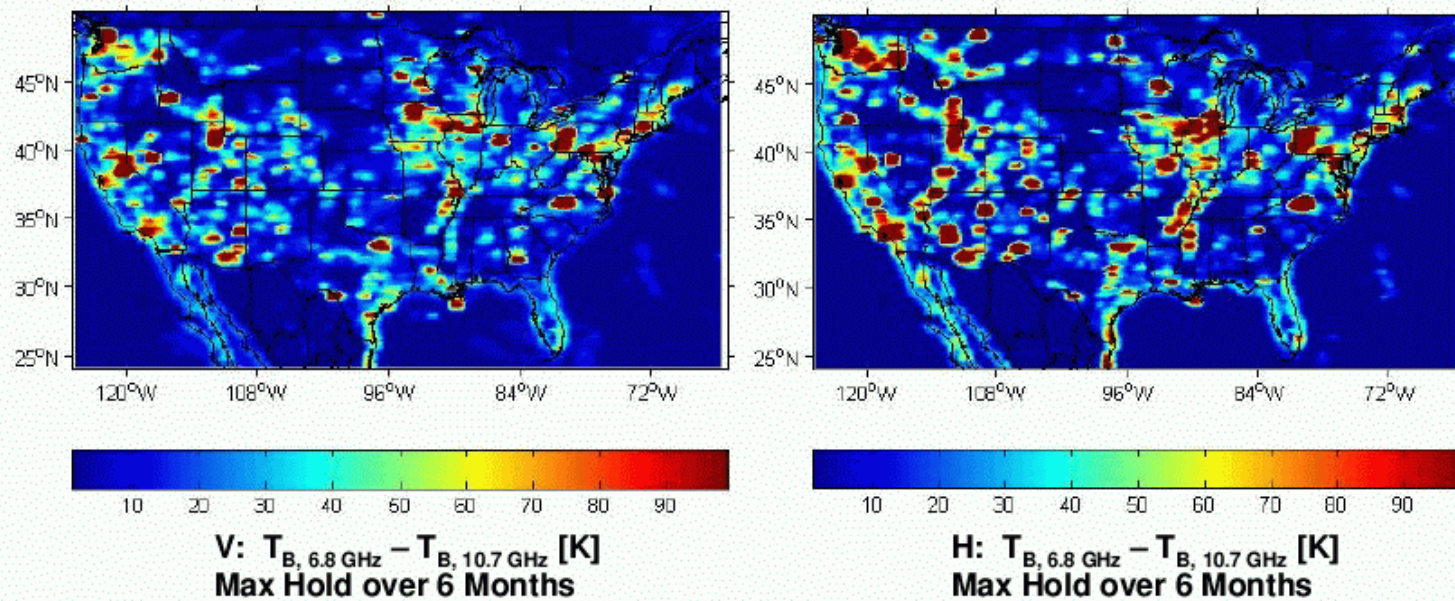


-1.0 -0.6 -0.2 0.2 0.6 1.0 [K]

-1.0 -0.6 -0.2 0.2 0.6 1.0 [K]

### “Spectral Index” $T_{B, 6.8 \text{ GHz}} - T_{B, 10.7 \text{ GHz}}$

- This index is nominally < 5 K (typically, negative) for the geophysical signal
- Values > 5K indicate RFI
- May be a more sensitive test for RFI than absolute  $T_B$ 's

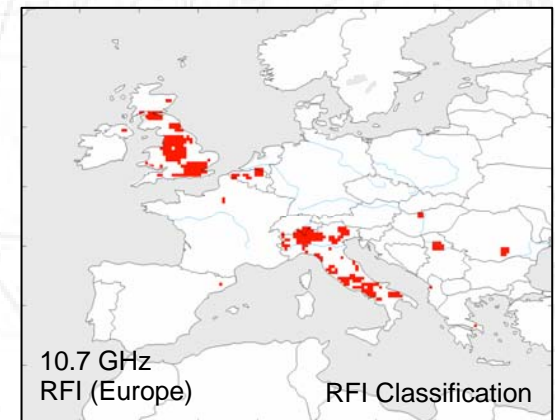
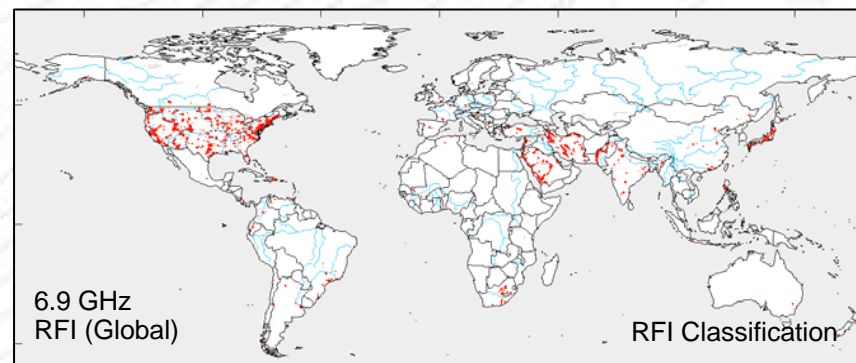
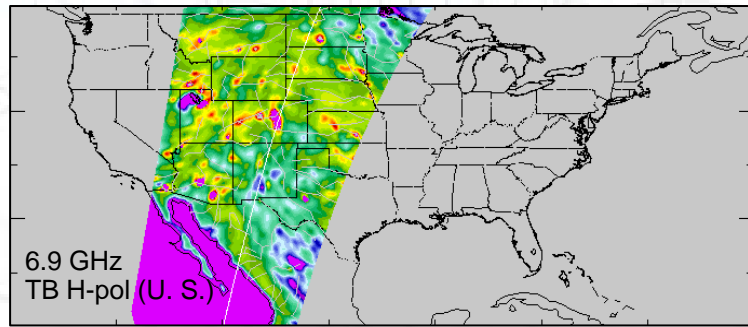


(Ellingson and Johnson 2004)

## Surface emission - RFI

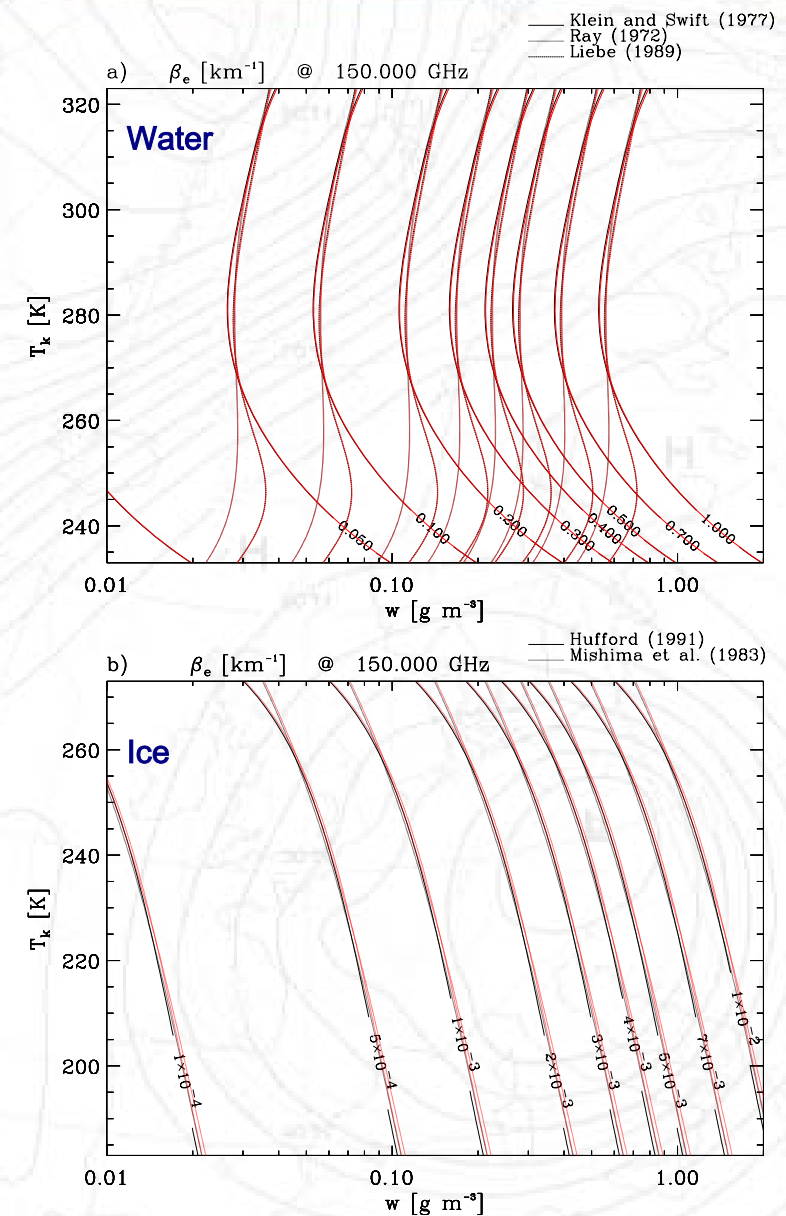
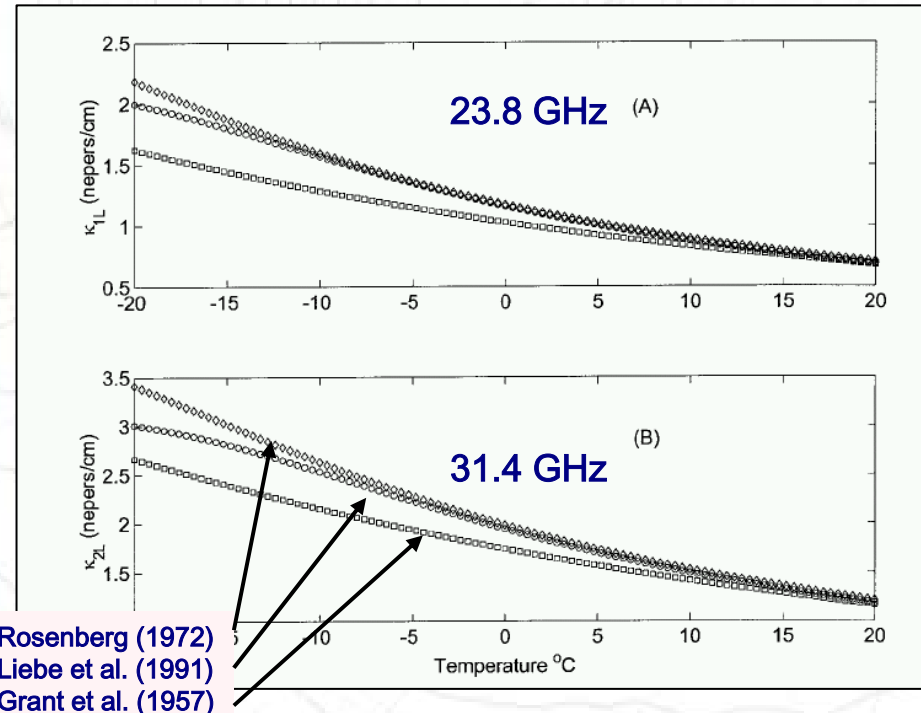
- RFI is observed in the AMSR C-band (6.75–7.1 GHz) and X-band (10.6–10.7 GHz) data
  - C-band is unprotected
  - X-band is protected from 10.68–10.7 GHz
- Classification algorithms can identify and filter strong RFI for AMSR-E geophysical algorithms
  - But, weak RFI cannot reliably be separated from geophysical signals
- C-band RFI mostly in the U. S., Japan, Middle East, some in Europe, Asia, S. America, Africa
- X-band RFI mostly in Japan, England, Italy, some in U. S.
- Situation at C-band has worsened considerably since Seasat and Nimbus-7 SMMR 1978-1987 (6.6 GHz)
- NPOESS/CMIS also operates at C- and X-bands
  - Re-assessment of radiometer design is in progress

(Njoku 2004)



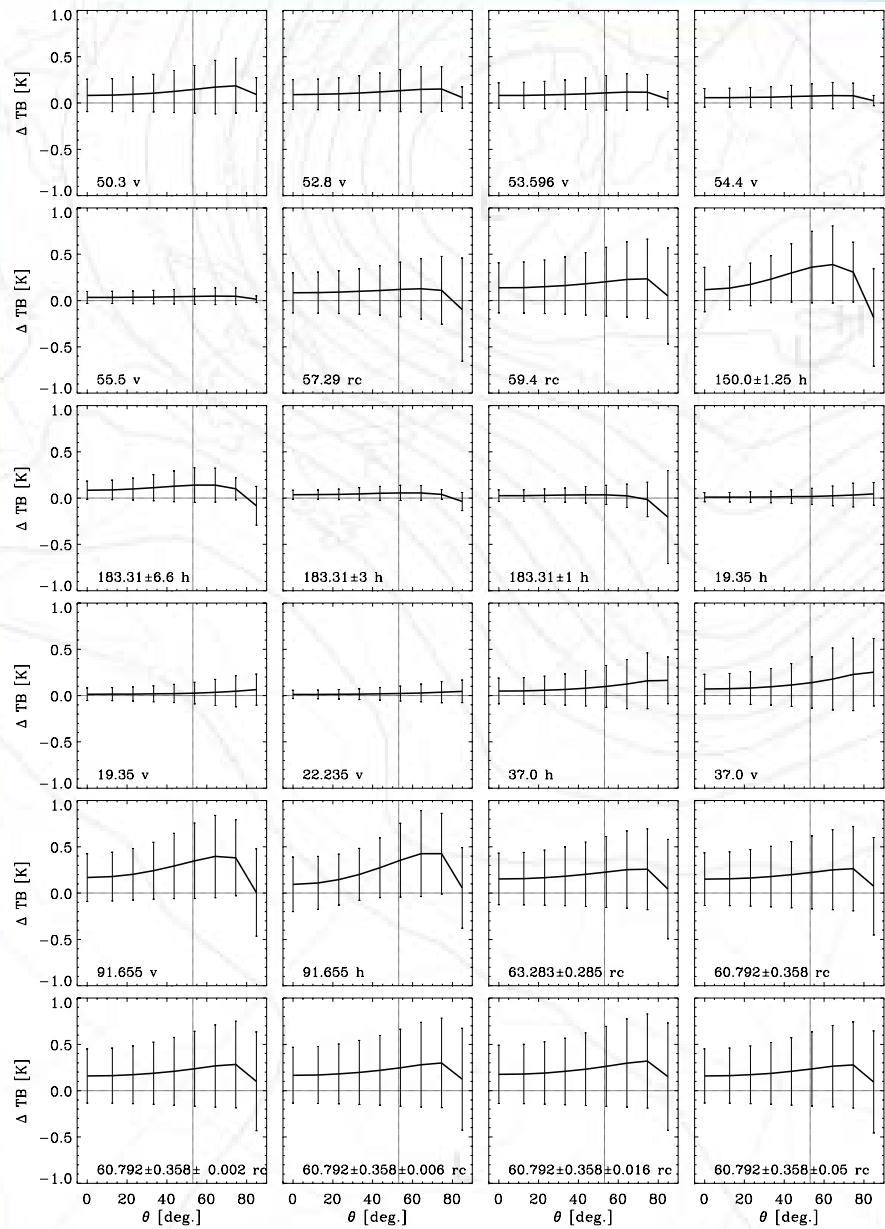
# Cloud water/ice absorption

Cloud water mass absorption coefficient,  $\kappa$ ,  
from various models  
(Westwater et al. 2001)



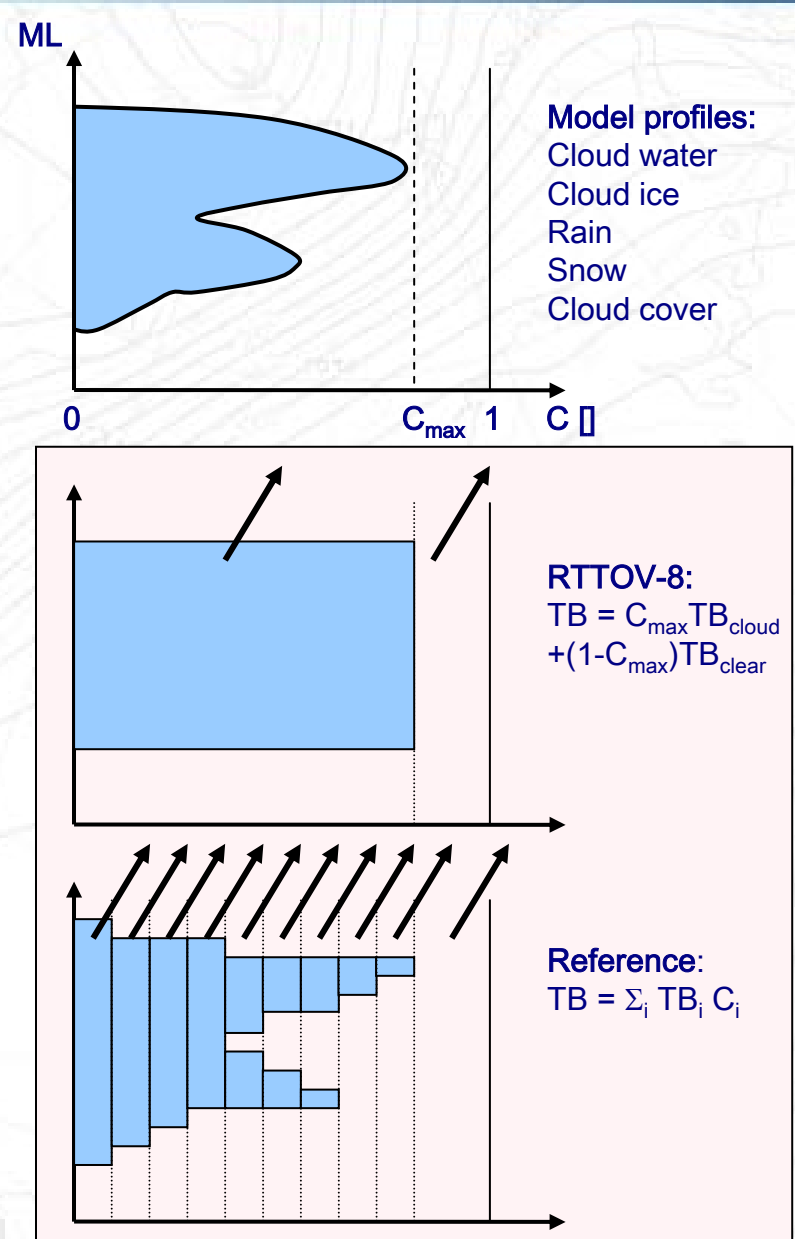
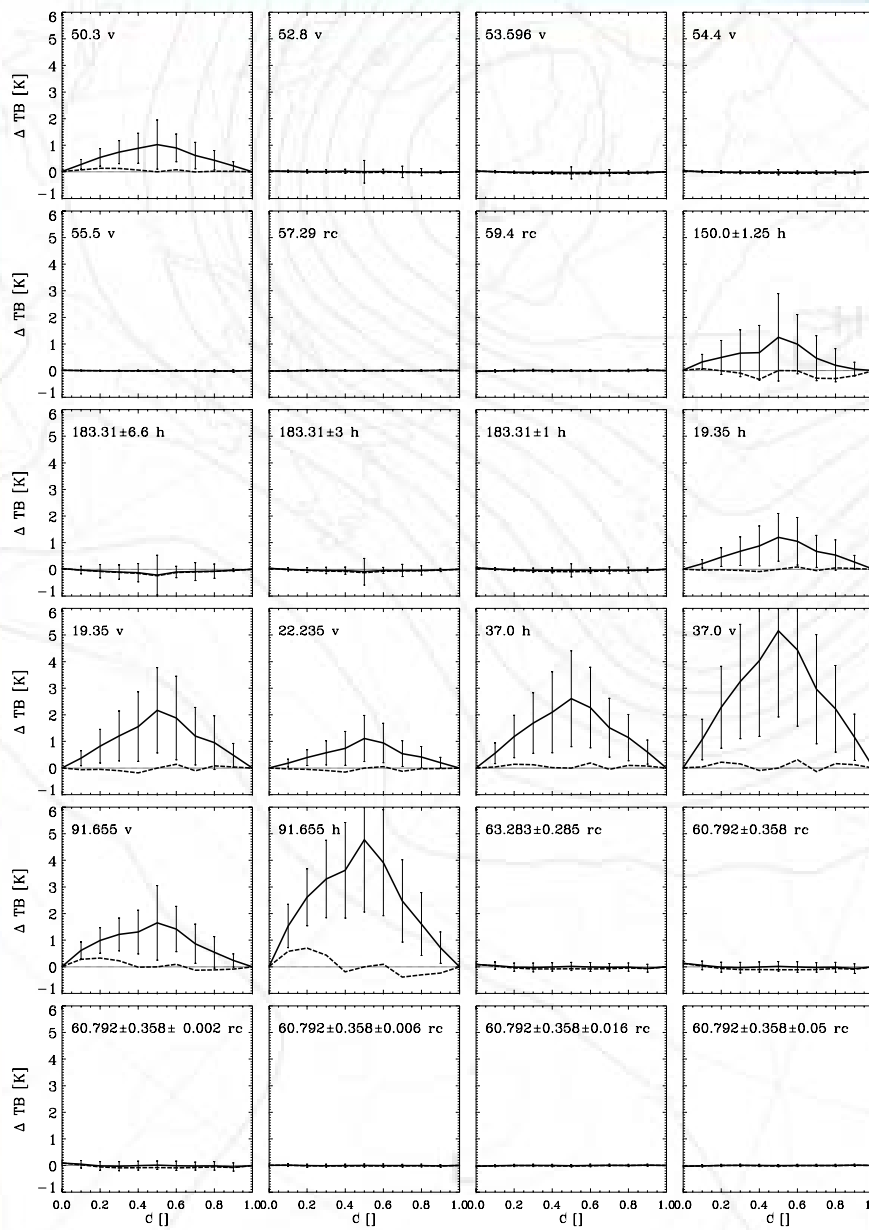
Cloud water/ice volume extinction coefficient ,  $\beta$ ,  
from various models and Rayleigh (black) and  
Mie (red) calculations at 150 GHz

## Multiple-scattering RT-Model comparison



RT-biases < 0.5 K!

## Effect of fractional cloud cover



## SSM/I TB FG/AN-Departures, September 2004

SSM/I channel:

1: 19.35 GHz (v)

2: 19.35 GHz (h)

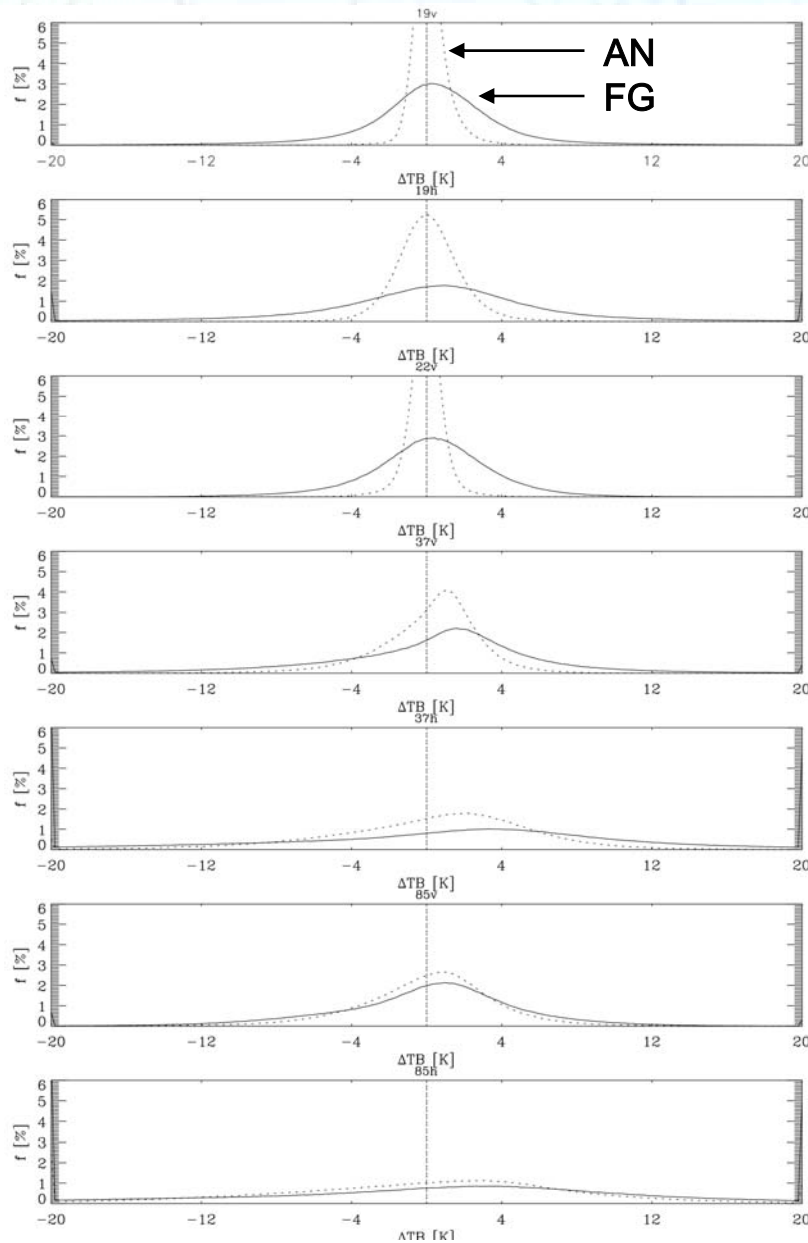
3: 22.235 GHz (v)

4: 37.0 GHz (v)

5: 37.0 GHz (h)

6: 85.5 GHz (v)

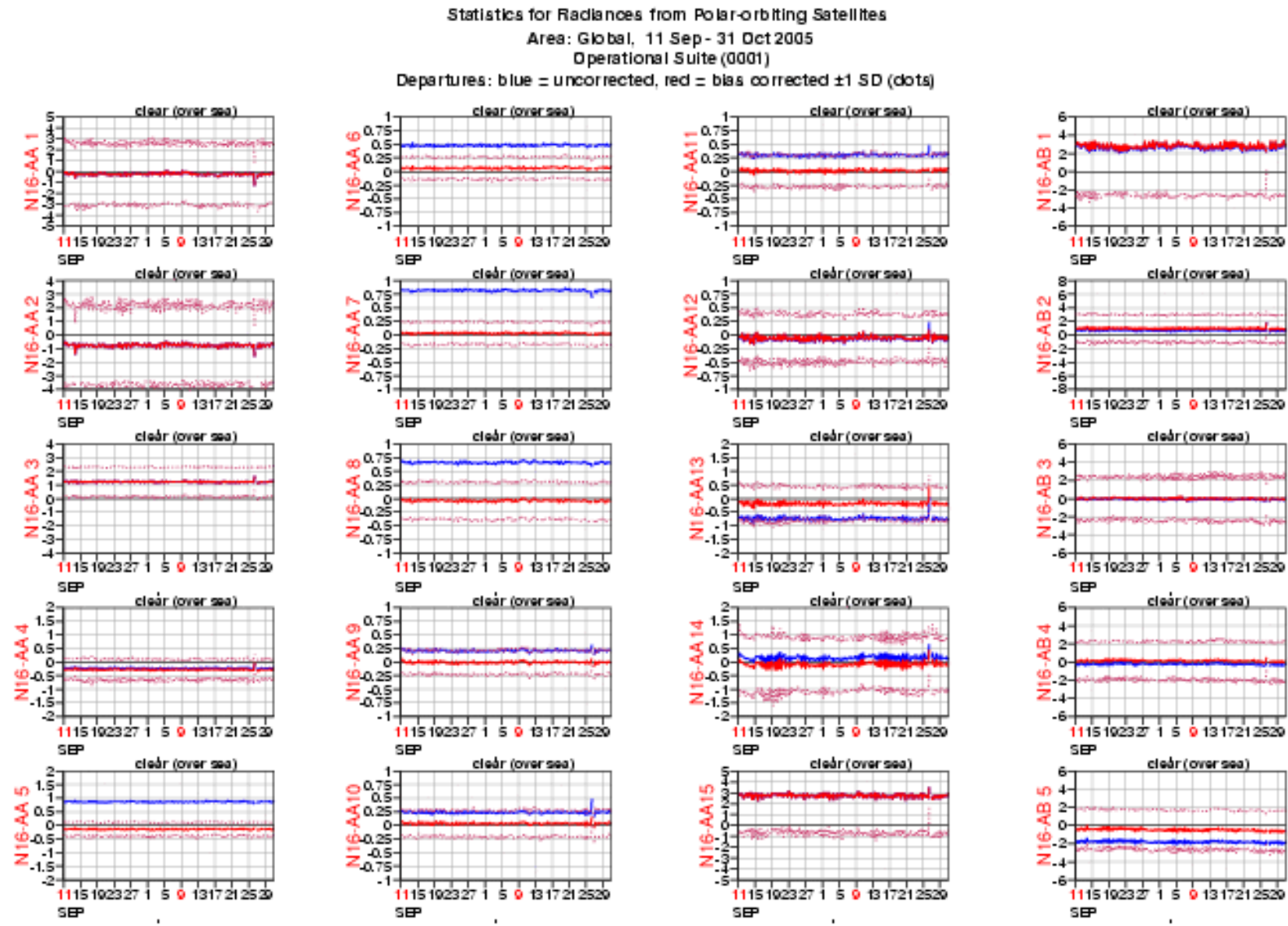
7: 85.5 GHz (h)



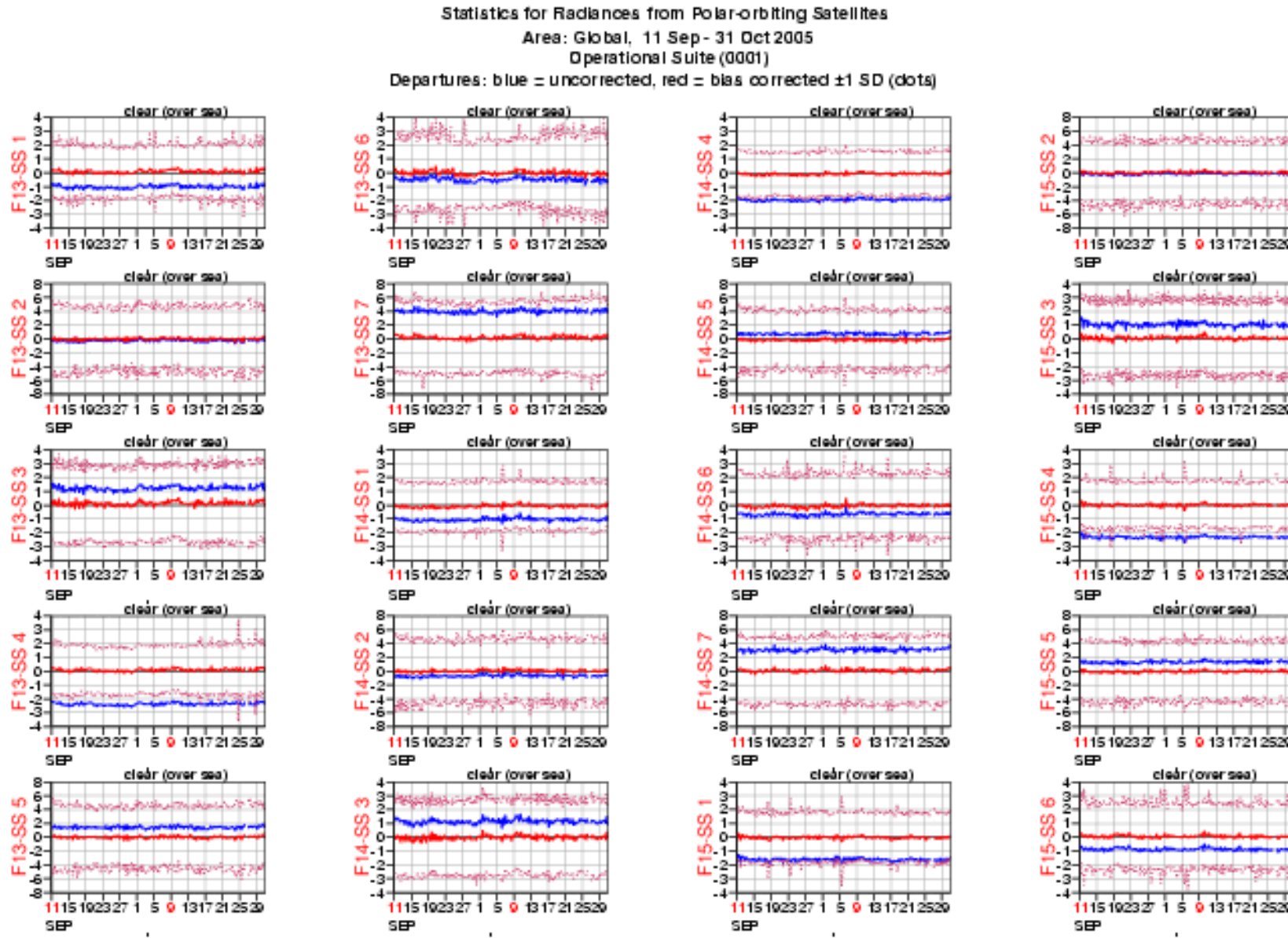
Bias corrected with  
TCWV-predictor only

Higher order effects  
(C-structure, PSD's etc.)  
become important

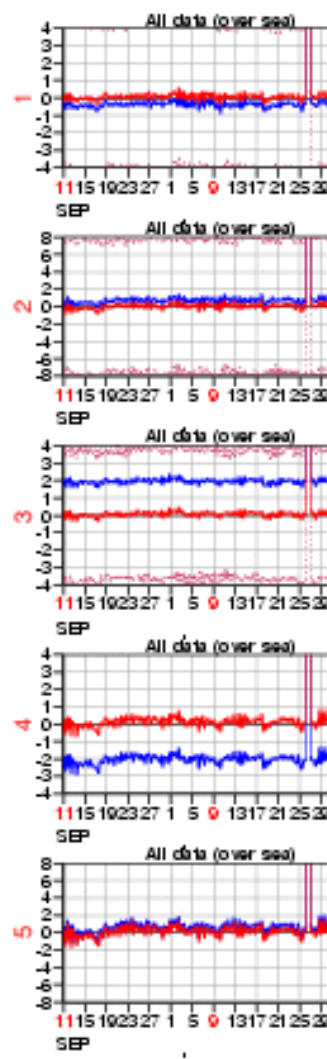
# Departure time series NOAA-16 AMSU-A/B (Clear-sky)



# Departure time series DMSP F-13/14/15 SSM/I (Clear-sky)



# Departure time series DMSP F-13/14/15 SSM/I (RAIN)

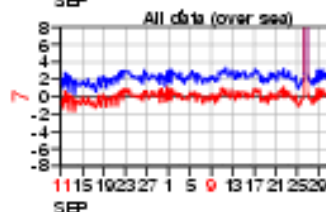
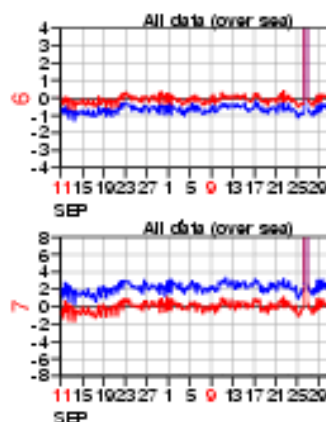


Statistics for Rain Affected Microwave Radiances from DMSP-11 / SSM/I

Area: Global, 11 Sep - 31 Oct 2005

Operational Suite (0001)

Departures: blue = uncorrected, red = bias corrected ±1 SD (dots)



## Summary



Contribution/Effect	Frequencies	Comments
<b>Atmospheric absorption:</b> Spectroscopy, LBL Parameterized models Zeeman splitting Faraday rotation	all all $O_2$ lines 1.4 20-300 GHz	$H_2O$ continuum problematic very accurate relative to LBL models limited applicability ( $p < 10$ hPa), SSMIS, MLS limited applicability, SMOS Clear-sky <i>atmospheric</i> TB's accurate within 1-3%
<b>Surface emission:</b> Sea surface Permittivity Polarimetry Land surfaces Soil, vegetation Snow/ice Type, age, etc.	all 10-37	1 K between 20-150 GHz 10% for $4 \text{ m/s} < \text{SWS} < 12 \text{ m/s}$
<b>Cloud droplet emission:</b> Permittivity	all 5-500 GHz	uncertain well modelled between 5-500 GHz and $T > 273$ K for $T < 273$ K models differ by 20-30%
<b>Precipitation emission/scattering:</b> PSD, Permittivity, Shape	all	uncertain
<b>Radiative transfer modelling:</b> Clear-skies Clouds/precipitation multiple scattering Layer inhomogeneity	all all	biases up to 3 K due to $T(z)$ , otherwise accurate biases < 0.5 K biases up to 5 K, can be parameterized